FEW-PHOTON TRANSPORT IN QUASI-ONE-DIMENSIONAL GEOMETRIES

by

Kevin Ralley

A thesis submitted to
The University of Birmingham
for the degree of
DOCTOR OF PHILOSOPHY

Theoretical Physics Group
School of Physics and Astronomy
College of Engineering and Physical Sciences
The University of Birmingham

September 2012

Abstract

An analysis of some aspects of photon transport through cavities and emitters embedded in a one-dimensional geometries is presented. The concept of photon blockade is defined for few-photon states interacting with a single two-level atom and the strength of achievable blockade is calculated in this setting. A brief review of some promising schemes for achieving photon blockade from the literature is also provided. The conflict between linear and nonlinear optical processes is studied for a novel version of the famous Hong-Ou-Mandel effect in a photonic waveguide with a side-coupled two-level emitter.

ACKNOWLEDGEMENTS

CONTENTS

LIST OF FIGURES

CHAPTER 1

INTRODUCTION

Under usual circumstances photons seldom interact. Effective interactions can be generated with the help of optically nonlinear materials although often intense light fields are required. It has been known since the earliest days of quantum optics that such interactions are often enhanced if the light field is confined to a restricted geometry [1], such as an optical cavity or a photonic waveguide. The last few decades have witnessed an explosive development of nano-fabrication techniques which has in turn stimulated a considerable amount of interest within the optical community concerning the transport properties of photons in these reduced dimensions [2, 3, 4, 5].

It is widely believed that the combined fidelity of light as a carrier of information and the newly discovered giant optical nonlinearities that can be achieved at the nano-scale make for the most promising route to harnessing the computational benefits that can be afforded at the quantum level [6, 7, 8]. Advances in this direction may also lead to a deeper insight into the fundamental interpretation of the quantum world. In particular it has been proposed that the cross-phase Kerr nonlinearities in certain crystals allow for non-demolition photon detection [9, 10].

All-optical devices, inspired by existing electrical analogues; that operate at ultra-low light intensities are now emerging from the vast body of research that has been invested. One of the most actively sought-after technologies is a single-photon transistor, that either transmits or reflects incident photons based on its interaction with another 'control' field. Photons are bosons and as such exhibit a tendency to arrive in bunches; for this reason isolating individual photons is especially challenging. A single-photon transistor would facilitate the conversion of a bunched incoming flux of light into anti-bunched, even single-photon pulses. In the mid-90s Imamoḡlu et al. [11] proposed a scheme that could harness the electromagnetically-induced-transparencies [12] achievable in a particular resonantly driven cavity-confined atom to generate giant optical nonlinearities with minimal losses. Photon transport through such a cavity is expected to proceed one-by-one in analogy with the more familiar Coulomb blockade effect found in electron transport through certain mesoscopic structures. This phenomenon, aptly named photon blockade has since been generated in a large variety of other settings [13, 14, 15, 16, 17], including in concert with Coulomb blockade [18].

The earliest observations of photon anti-bunching were made in the resonant fluorescence from a two-level transition in a single atom. The origin of this anti-bunching in the scattered field is well understood [19]; a single photon absorbed from the incident flux promotes an atomic electron to the excited level. After some time the atom decays and following this transition there is a zero probability that another photon will be scattered until the electron is again promoted to the excited level. Consequently the scattered photons will be temporally anti-bunched for intervals shorter than the characteristic atom decay time [20]. One of the original contributions made in this thesis is an exact calculation of the strength of photon blockade that can be achieved for few-photon pulses with a single atom when the light field is constrained to just one dimension.

The interaction of a light field confined to one dimension with a single two-level emitter at optical frequencies is well described by the Dicke Hamilton [21]. The early sections of this thesis are devoted to extracting the few-photon eigenstates for this model. Once the complete set has been found the multi-photon scattering states in principle follow for arbitrary initial configurations and turn out to be remarkably simple [22]. In the chiral case, where all photons travel in one particular direction only, the evolution of each photon proceeds independently of all others except for the deletion of photon paths where double occupation of the emitter is implied.

A number of optical phenomena do not yield to a classical or semi-classical explanation a classic example is the Hong-Ou-Mandel effect [23], which refers to the observation that two photons with identical spectral composition and polarization arriving simultaneously at a balanced beamsplitter from distinct incoming ports are always found exiting together in one of the two possible outgoing ports. The coalescence of the two photons is attributed to a quantum interference between possible photon paths. The second original contribution made by this thesis is to determine the reduction in interference visibility that is suffered when a single two-level atom replaces the usual (linear) beamsplitter in a one-dimensional analogue of the Hong-Ou-Mandel geometry.

CHAPTER 2

MULTI-PHOTON SCATTERING THROUGH A TWO-LEVEL ATOM

2.1 Introduction

One of the simplest light-matter interactions conceivable is that of a light field nearly resonant with a two-level atomic transition. If the characteristic wavelength of the incident radiation is much longer than the atomic diameter then the dipole approximation can be made and the following Hamiltonian becomes responsible for the dynamics:

$$\hat{H} = \hat{H}_R + \hat{H}_A + \hat{\mathbf{d}} \cdot \hat{\mathbf{E}} \left(\mathbf{r} = \mathbf{0} \right). \tag{2.1}$$

$\hat{H}_R$ and $\hat{H}_A$ encode for the free motion of the radiation and the two-level atom respectively; their mutual interaction is described by the final term. The dipole operator $\hat{\mathbf{d}}$ contributes no diagonal matrix elements in the basis of the atomic states and consequently $\hat{\mathbf{d}} = \mathbf{d}\hat{S}^+ + \bar{\mathbf{d}}\hat{S}^-$ with $\mathbf{d} = \langle e| \hat{\mathbf{d}} |g \rangle$ and where $\hat{S}^+$ is the pseudo spin-1/2 raising operator connecting the ground state of the emitter with its excited state, that is $\hat{S}^+ = |e\rangle\langle g|$. In the long-wavelength limit only the amplitude of the electric field at the position of the atom, which for convenience is set to be at the origin is relevant. Many more gauge-equivalent representations exist for the

light-atom interaction but the above is most convenient for the current purposes.

Expanding the electric field into its normal modes and writing $\hat{H}_R$ and $\hat{H}_A$ explicitly provides

$$\hat{H} = \omega_{12}\hat{S}^z + \sum_{\mathbf{k},\mu} \omega_{\mathbf{k},\mu} \, \hat{a}^+_{\mathbf{k},\mu}\hat{a}_{\mathbf{k},\mu} + \sum_{\mathbf{k},\mu} g_{\mathbf{k},\mu} \, (\hat{S}^+ + \hat{S}^-)(\hat{a}^+_{\mathbf{k},\mu} + \hat{a}_{\mathbf{k},\mu}), \qquad (2.2)$$

where ω_{12} is the atomic energy level spacing and $\mathbf{k}$ and μ refer to the momentum and polarization of the radiation respectively. The coupling constant $g_{\mathbf{k},\mu}$ can be chosen to be real, and is the magnitude of the product of the radiation mode functions taken at the origin and the dipole matrix element. A perturbative expansion in the interaction generates contributions in increasing inverse powers of $\omega_0 - \omega_{\mathbf{k}}$ and $\omega_0 + \omega_{\mathbf{k}}$. The first term corresponding to energy conserving processes such as the creation of a photon at the expense of a de-excited emitter $\hat{a}^+_{\mathbf{k},\mu}\hat{S}^-$ and vice-versa. Stimulated and spontaneous emission are examples of such processes while the second term relates to virtual processes such as the simultaneous excitation of the emitter and the creation of a photon, $\hat{a}^+_{\mathbf{k},\mu}\hat{S}^+$+ h.c. At optical frequencies and near resonance, processes of the first type dominate and the others can be neglected, this elimination is often referred to in the literature as the rotating-wave approximation [24].

Throughout this thesis the light field will be repeatedly considered in one dimension; this will either be because only s-wave scattering is relevant or else the field is restricted to one dimension by some confining geometry. After linearizing the photon spectrum, measuring all energies with respect to the energy-level spacing and taking the value of the coupling strength at resonance the Dicke Hamiltonian is derived. The aim of the current chapter is to extract the multi-photon scattering eigenstates of this Hamiltonian so they can be used in later sections to determine few-photon transport characteristics in various geometries.

2.2 Eigenstates of the Multimode Dicke Hamiltonian

The one-dimensional multi-mode chiral Dicke Hamiltonian [21] can be represented as

$$\hat{H} = -i \int dx \, \hat{a}^+ (x) \, \partial_x \, \hat{a} (x) - \sqrt{\gamma} \left[\hat{S}^+ \hat{a} (0) + \hat{a}^+ (0) \, \hat{S}^- \right]. \tag{2.3}$$

It belongs to the set of integrable models and its exact many-body eigenstates are given in the form of a Bethe ansatz. This chapter introduces the Bethe ansatz and determines these states explicitly. In the context of photon scattering these fully interacting eigenstates can then be used to construct the many-body S-matrix. An essential property of the Hamiltonian (2.3) that facilitates its integrability is that it preserves the total number of excitations represented by the operator

$$\hat{N} = \int dx \, \hat{a}^+ (x) \, \hat{a} (x) + \hat{S}^+ \hat{S}^-. \tag{2.4}$$

This means that each particle number subspace can be diagonalized independently since they are not coupled to one another by the interaction. The most general n-body state is

$$\begin{aligned} |\psi_n\rangle &= \int d^n x \, g_n (x_1, \ldots, x_n) \, \hat{a}^+ (x_1) \ldots \hat{a}^+ (x_n) \, |\rangle \\ &+ \int d^{n-1} x \, e_n (x_1, \ldots, x_{n-1}) \, \hat{a}^+ (x_1) \ldots \hat{a}^+ (x_{n-1}) \, \hat{S}^+ \, |\rangle, \end{aligned} \tag{2.5}$$

where the vacuum $|\rangle$ refers to the state containing no excitations, that is 0 photons, and the atom in its lowest level; $\hat{N} |\rangle = 0$. The requirement that (2.5) be an eigenstate of the Hamiltonian, $\hat{H} |\psi_n\rangle = E_n |\psi_n\rangle$, translates into the following set of equations

$$\begin{aligned} \left[-i \left(\partial_{x_1} + \cdots + \partial_{x_n} \right) - E_n \right] g_n (x_1, \ldots, x_n) & \\ - \frac{\sqrt{\gamma}}{n} \left[\delta (x_1) \, e_n (x_2, \ldots, x_n) + \cdots + \delta (x_n) \, e_n (x_1, \ldots, x_{n-1}) \right] &= 0, \qquad (2.6) \\ \left[-i \left(\partial_{x_1} + \cdots + \partial_{x_{n-1}} \right) - E_n \right] e_n(x_1, \ldots, x_{n-1}) - n\sqrt{\gamma} \, g_n (0, x_1, \ldots, x_{n-1}) &= 0. \end{aligned}$$

6

The first of these generates a series of discontinuities in the wavefunction, $g_n(x_1, \ldots, x_n)$; at the site of the two-level impurity, $x_i = 0$, $i = 1, 2, \ldots, n$. The frequency-independence of the coupling (an artefact of the resonance approximation) means that at these discontinuities the value of the photon wavefunction is not properly defined. This ambiguity is fixed by the additional definition $g_n(0, x_2, \ldots, x_n) = [g_n(0^-, x_2, \ldots, x_n) + g_n(0^+, x_2, \ldots, x_n)]/2$ which extends to all other coordinates by virtue of Bose symmetry.

2.2.1   Single-Particle Eigenstate

In the single-excitation sector the equations (2.6) admit a solution of the form

$$g_k(x) = e^{ikx} f_k(x), \quad f_k(x) = \theta(x < 0) + s_k\, \theta(0 < x), \quad s_k = \frac{k - i\gamma/2}{k + i\gamma/2}, \qquad (2.7)$$

with corresponding energy $E_1 = k$. Throughout this thesis the notation $\theta(x_1 < x_2 < \cdots x_n) \equiv \theta(x_n - x_{n-1}) \cdots (x_3 - x_2)\, \theta(x_2 - x_1)$ is adopted so that wavefunctions, which become more complicated with larger numbers of excitations, may be written clearly and compactly. The above state reveals that the effect of the emitter is to impart a phase-shift to the passing photon. Taking (2.7) together with the connection between the atomic-excitation amplitude and the photon wavefunction, $e_k = -\sqrt{\gamma} g_k(0)/k$, it is straightforward to demonstrate the following more compact representation of the single-particle eigenstates

$$|k+\rangle = N_1 \int dx\, e^{ikx} f_k(x)\, \hat{r}_k^+(x)\, |\rangle, \qquad (2.8)$$

where N_1 is set by normalization. The '+' included in the labeling of (2.8) indicates that it is a fully-interacting eigenstate, distinguishing it from the free-photon plane-waves that will be referred to later and will be denoted by $|k_n, \ldots, k_1\rangle = \hat{a}_{k_n}^+ \cdots \hat{a}_{k_1}^+ |\rangle$. This notation will be especially useful when asymptotic scattered states are introduced. The single-excitation

operator is defined by

$$\hat{r}_k^+ (x) = \hat{a}^+ (x) - \frac{\sqrt{\gamma}}{k} \delta (x) \hat{S}^+. \tag{2.9}$$

Many-particle eigenstates defined by the system (2.6) are much more difficult to derive, before presenting them it is necessary to give a brief review of the Bethe ansatz and its application to the current problem.

2.2.2 Bethe Ansatz

In a groundbreaking 1931 paper, Bethe outlined a procedure that could generate the complete and exact set of many-body eigenstates for a spin-1/2 periodic Heisenberg chain of arbitrary length [25]. Each spin belonging to such a chain is projected either parallel or antiparallel to a chosen quantization axis and the relative number of up and down spins is preserved despite the Heisenberg interaction acting between nearest neighbours, $\hat{H} = -J \sum_i \hat{S}_i \cdot \hat{S}_{i+1}$. The ferromagnetic case, $J > 0$, favours parallel spins, in this case the state with all spins down which may be interpreted as a sort of vacuum out of which particle-like excitations are created, each corresponding to an inverted spin. With negative spin-coupling, $J < 0$, antiferromagnetic spin ordering is preferred and a corresponding vacuum state exists. Single quasi-particle eigenstates are then represented by translation-symmetric plane-waves, their energies parameterized by a wavenumber k which is quantized by the finite length of the chain into units of the first periodicity-allowed non-zero k-point, $2\pi/L$. The many-particle eigenstates and eigenenergies are complicated by interaction and although in principle they can be extracted with a brute force diagonalization of the Hamiltonian in each disconnected particle-number subspace this naive approach soon becomes numerically intractable with the increasing size of each subspace. Bethe's penetrating insight was to point out that when only one particle belongs to each site the wavefunction is simply a product of single-particle plane-waves defined by a conserved set of quasi-momenta. In addition, scattering phase-shifts

develop in this state whenever two adjacent particles exchange locations. Enforcing periodic boundaries on the Bethe ansatz leads to a series of equations that determine the permissible values of quasi-momenta. It can be shown that describing the many-body eigenstates of the Heisenberg model in this way accounts for the entire spectrum.

This remarkable observation went largely ignored for over 30 years until in 1963 Lieb and Liniger applied a similar ansatz to solve a one-dimensional model of spinless delta-function interacting bosons [26]. Their result generated a surge of interest and prompted the discovery of many more non-trivial exactly solvable one-dimensional problems from almost all areas of theoretical physics (some examples can be found in [27] and references cited therein). In 1982 Rupasov found that the chiral Dicke Hamiltonian (2.3) also belongs to this set of integrable models [28] in one of only a few instances where the Bethe ansatz has been employed in a scattering context in contrast to its traditional thermodynamic setting.

Just as for the Heisenberg chain and Lieb-Liniger gas; the many-body eigenstates of the Dicke model come in the form of superpositions of plane waves; the only additional feature is a series of phase-shifts that are acquired by photons as they scatter past the two-level impurity. These impurity-induced phase shifts are encoded in the functions $f_k(x)$ which are defined in (2.7). Specifically, an n-photon eigenstate in the ordered sector $x_1 < x_2 \cdots < x_n$ has the following representation

$$g_{k_1,\ldots,k_n}(x_1,\ldots,x_n) = \sum_P A(P_1 \ldots P_n) f_{k_{P_1}}(x_1) \ldots f_{k_{P_n}}(x_n) e^{ik_{P_1}x_1 + \cdots + ik_{P_n}x_n}, \qquad (2.10)$$

the set P includes all permutations of the integers $1, \ldots, n$. The state in the remaining $n! - 1$ regions corresponding to alternative particle orderings is determined by Bose-symmetry. It will be shown that the requirement that the above ansatz be a properly normalized eigenstate

of the Hamiltonian (2.3) happens to be sufficient to uniquely fix all of the amplitudes $A(P)$.

A characteristic feature of Bethe-solvable models is that they incorporate an infinite number of independent constants of motion. These constants are often difficult to determine but their existence in the case of the Dicke model forces the magnitude of every amplitude $A(P)$ to be equivalent; moreover, those that differ by permutations of adjacent indices are related by two-particle scattering phases. The magnitude of every amplitude is then determined by the normalization requirement. Physically an infinite set of hidden symmetries conspire to render all interactions effectively pairwise, particles become limited to merely exchanging quasi-momenta and in this sense scattering is non-diffractive.

Applying suitable boundary conditions to the photon wavefunction (2.10) will determine the allowed values of quasi-momenta (or rapidities) which in turn specify the energy of each state, $E_n = k_1 + k_2 + \cdots + k_n$. It is worth emphasizing that they are not the actual momenta carried by the individual photons and with interaction many of them will become complex-valued, clustered in groups of conjugate pairs corresponding to bound multi-photon states. Periodic boundaries are typically used in conjunction with the Bethe ansatz although open boundaries are more suited to scattering problems. Here for convenience the permissible rapidities are extracted according to conventional periodic boundaries and afterwards this unphysical assumption is relaxed by extending the system size to infinity where boundary effects are expected to be exponentially suppressed. This approach is not generally valid and a justification is necessary a posteriori. For some models, especially in an out-of-equillibrium context, the correct choice of boundary conditions remains essential even in the above limit and an extension of the Bethe ansatz is currently being developed to deal with such cases [29].

The relationship between so many exactly solvable models is intriguing yet, despite many

attempts, a general method for predicting integrability has remained elusive. The only real progress in this direction came with the discovery of the Yang-Baxter equations (YBEs) which make it possible to unambiguously demonstrate that certain models do not permit a solution of the Bethe ansatz sort. Initially formulated by Yang [30] as a consistency criterion for the multi-component repulsive Bose gas, their ubiquity in the context of integrability was soon realised by Baxter who applied them while calculating the exact free energy of the six- and eight-vertex models of statistical mechanics (amongst others) [31, 32]. A general feature of Bethe-integrable models is the complete factorization of the many-body interactions that they describe into sequences of two-body scatterings. It is therefore essential for consistency that these sequences be unique and this requirement is the content of the YBEs. In practice, given a particular model its amenability to a Bethe solution is determined by extracting its two-body scattering matrices by any available method; once found they can then be entered into the YBEs and if they are found to be consistent then it is possible, but not guaranteed that a Bethe ansatz solution exists. If they do not satisfy the YBEs then the model certainly does not permit a solution of the Bethe type, irrespective of whether or not it is integrable.

2.2.3 Two-Particle Eigenstate

The solution of problem (2.6) for two particles provides the essential irreducible scattering matrices for the Dicke Model. This task is achieved most directly by postulating the following representation for the photon wavefunction:

$$g_{k_1,k_2}(x_1, x_2) = \sum_P A(P_1 P_2) f_{k_{P_1}}(x_1) f_{k_{P_2}}(x_2) e^{ik_{P_1} x_1 + ik_{P_2} x_2}, \tag{2.11}$$

expressed in the region $x_1 < x_2$. The first equation in (2.6) provides a connection between the wavefunction (2.11) and the atomic-excitation amplitude, that is

$$e_2(x) = \frac{-2i}{\sqrt{\gamma}} \left[g_2(0^+, x) - g_2(0^-, x) \right] = \frac{-2i}{\sqrt{\gamma}} \left[g_2(x, 0^+) - g_2(x, 0^-) \right], \tag{2.12}$$

and the requirement that this amplitude be single-valued at the origin,

$$e_2(0^+) = e_2(0^-), \tag{2.13}$$

translates into a continuity condition for the field at the location of the emitter

$$g_2(0^+, 0^+) - g_2(0^-, 0^+) = g_2(0^-, 0^+) - g_2(0^-, 0^-), \tag{2.14}$$

which in turn establishes a connection between the amplitudes $A(12)$ and $A(21)$. Combining the relations (2.11) and (2.14) reveals that

$$A(12) = Y_{12} A(21), \quad A(21) = Y_{21} A(12), \quad Y_{ij} = \frac{k_i - k_j - i\gamma}{k_i - k_j + i\gamma}; \tag{2.15}$$

these are the required two-body scattering matrix elements. The Bethe ansatz (2.11) and the connections between the amplitudes (2.15) specify a general two-particle eigenstate of

the Dicke Hamiltonian (2.3) with corresponding energy $E_2 = k_1 + k_2$. The state can be represented more compactly as

$$|k_2, k_1+\rangle = N_2 \int d^2x \left[\theta\left(x_2 < x_1\right) + Y_{12}\,\theta\left(x_2 > x_1\right)\right] \prod_{j=1,2} f_{k_j}\left(x_j\right) e^{ik_j x_j}\, \hat{r}_{k_j}^+\left(x_j\right)|\rangle, \quad (2.16)$$

establishing contact with the result (2.8) for a single particle and revealing the significance of the phase Y_{12} acquired by the state as the photons pass one another. This phase-shift alone does not necessarily imply any effective interaction between the two photons since it persists even when they are far from the scattering center, in fact it can be easily shown that for arbitrary Y_{12} the symmetrized two-photon wavefunction satisfies

$$-i(\partial_{x_1} + \partial_{x_2})\, g_{k_2,k_1}(x_1, x_2) = E_2\, g_{k_2,k_1}(x_1, x_2), \qquad x_1, x_2 \neq 0. \qquad (2.17)$$

In general it can be shown that free particles with linear dispersion permit representations with arbitrary phase-shifts [33]; the introduction of an impurity simply lifts this degeneracy. Such phase-shifts are encountered in the solutions to both the Kondo [34] and more generally the Anderson impurity problems [35].

It remains to be shown that all possible two-particle eigenstates of the Dicke Hamiltonian are accounted for by the representation (2.16). The general complexity of Bethe states makes confirming their completeness a challenging task and this issue has led to some apparent contradiction in the literature [36, 37, 22]. A group of authors have asserted that at least for two photons the Bethe states are not complete and that a two-photon bound state has to be included to render them so. The following short section demonstrates that by applying periodic boundaries to the general state (2.16) the bound state they suggest arises naturally.

Complex Rapidities and the Two-Photon Bound State

Confining the system to a ring of length L, periodicity implies that $g_2(-L/2, x) = g_2(L/2, x)$ and $g_2(x, -L/2) = g_2(x, L/2)$ which limits the allowed rapidities to those that satisfy the following relations

$$e^{ik_jL}s_{k_j} = Y_{ji} \rightarrow e^{ik_jL}\frac{k_j - i\gamma/2}{k_j + i\gamma/2} = \frac{k_j - k_i - i\gamma}{k_j - k_i + i\gamma}, \quad i \neq j. \tag{2.18}$$

In addition to real solutions the above requirements do not exclude the existence of complex quasi-momenta. The energy, $E_2 = k_1 + k_2$ however must be real and as a consequence, $\text{Im}\{k_1\} = -\text{Im}\{k_2\}$. In the limit of infinite system size only one complex valued solution is permitted, $k_1 = (E_2 + i\gamma)/2$ and $k_2 = (E_2 - i\gamma)/2$ that define a properly bounded eigenstate. Substituting them into general wavefunction (2.11) and writing the resulting state in the outgoing region $0 < x_1, x_2$ reveals

$$g_2^B(x, X_c) = \frac{E_2 - 2i\gamma}{E_2 + 2i\gamma}e^{iE_2X_c}e^{-\gamma|x|/2}, \tag{2.19}$$

represented in terms of the centre-of-mass coordinate of the photons, $X_c = (x_1 + x_2)/2$, and their relative coordinate, $x = x_2 - x_1$, in order to emphasise its bound character. The amplitude of the state clearly diminishes with increasing photon separation. The state (2.19) is identical to the one obtained by more careful considerations elsewhere [36, 37] with open boundaries.

2.2.4 Three-Particle Eigenstate and the Yang-Baxter Equations

The three-body problem represents the first non-trivial application of the Bethe ansatz to the Dicke model; the absence of three-body scattering here is essential for the validity of the ansatz. The relevant photon state expressed in the ordered region $x_1 < x_2 < x_3$ is

$$g_{k_1,k_2,k_3}(x_1,x_2,x_3) = \sum_P A(P_1 P_2 P_3) f_{k_{P_1}}(x_1) f_{k_{P_2}}(x_2) f_{k_{P_3}}(x_3) e^{ik_{P_1}x_1 + ik_{P_2}x_2 + ik_{P_3}x_3}. \quad (2.20)$$

Once again the first equation in (2.6) connects the photon state with the atomic excitation amplitude. Continuity of this amplitude on passing the origin

$$e_3(0^+,0^+) = e_3(0^-,0^+) = e_3(0^-,0^-), \quad (2.21)$$

amounts to the following restrictions on the three-photon wavefunction

$$g_3(0^+,0^+,0^+) - g_3(0^-,0^+,0^+) = g_3(0^-,0^+,0^+) - g_3(0^-,0^-,0^+)$$
$$= g_3(0^-,0^+,0^-) - g_3(0^-,0^-,0^-). \quad (2.22)$$

A quick check by direct substitution will confirm that this requirement is met when all $A(P)$ differing by a pairwise permutation of neighboring photons are related by the same two-body phase defined in the previous section, that is when $A(ijk) = Y_{ij}A(jik) = Y_{ij}Y_{ik}A(jki)$ and so forth. For four or more particles continuity conditions similar to (2.22) continue to arise, each satisfied when the amplitudes in each ordered sector are related by the two-body phases (2.15). In other words, it appears that a class of n-body eigenstates of (2.3) exist that are representable in the form of a Bethe ansatz characterized by a set of $n!$ amplitudes $A(P_1, P_2, \ldots, P_n)$ such that for each pair differing by a single permutation of adjacent P

labels, the following linear dependence is observed

$$A\left(\ldots P_{i+1}, P_i \ldots\right) = Y_{P_{i+1}P_i} A\left(\ldots P_i, P_{i+1} \ldots\right). \tag{2.23}$$

There are $n!\left(n-1\right)/2$ such connections which, for more than two particles, exceeds the number of amplitudes that they define; mutual consistency is then ensured by the YBEs. For identical particles they simply amount to the requirements

$$Y_{ij}Y_{ji} = 1, \qquad Y_{ij}Y_{ik}Y_{jk} = Y_{jk}Y_{ik}Y_{ij}. \tag{2.24}$$

The first guarantees that permuting any pair of adjacent particles an even number of times does not alter the state while the second is a sufficient condition ensuring the uniqueness of all scattering factorizations. YBEs similar to those in (2.24) for the more general case of distinguishable particles can be derived and are far more restrictive [34, 35]. Substituting the known two-body scattering phases for the Dicke Model (2.15) into the Yang-Baxter equations (2.24) confirms their consistency, indicating that the states (2.20) represent a set of exact three-body eigenstates.

2.2.5 Many-Particle Eigenstates

The findings of the preceding sections lead to the conclusion that a class of many-body eigenstates exists for the Dicke model that may be written in the form [33, 38, 39]

$$|k_1, \ldots, k_n+\rangle = N_n \int d^n x \prod_{i<j} \left[\theta\left(x_j < x_i\right) + Y_{ij}\,\theta\left(x_j > x_i\right)\right] \prod_j f_{k_j}\left(x_j\right) e^{ik_j x_j}\, \hat{r}_{k_j}^+\left(x_j\right)|\rangle. \tag{2.25}$$

Applying the Dicke Hamiltonian (2.3) to the states (2.25) directly confirms their status as eigenstates, $\hat{H}\,|k_1, \ldots, k_n+\rangle = E_n\,|k_1, \ldots, k_n+\rangle$ with corresponding energies given by the

16

sum of their rapidities $E_n = k_1 + k_2 + \cdots + k_n$. The square brackets incorporate the only non-factorizable terms that encode the entanglement developed between photons as a result of their mutual interaction with the two-level impurity.

It can be shown that in the infinite-system-size limit all allowed quasi-momenta that are consistent with periodicity come in the form of strings of two or more linked by a common real component (or principal rapidity) [25]. To illustrate this point the solution to the four-photon problem results in a sets of allowed rapidities each belonging to one of the five possible configurations:

$$
\begin{aligned}
(i): \quad & k_1 = \kappa_1^i, \ k_2 = \kappa_2^i, \ k_3 = \kappa_3^i, \ k_4 = \kappa_4^i, \\
(ii): \quad & k_1 = \kappa_1^{ii}, \ k_2 = \kappa_2^{ii}, \ [\, k_3 = \kappa_3^{ii} + i\gamma/2, \ k_4 = \kappa_3^{ii} - i\gamma/2 \,], \\
(iii): \quad & [\, k_1 = \kappa_1^{iii} + i\gamma/2, \ k_2 = \kappa_1^{iii} - i\gamma/2 \,], \ [\, k_3 = \kappa_2^{iii} + i\gamma/2, \ k_4 = \kappa_2^{iii} - i\gamma/2 \,], \quad (2.26) \\
(iv): \quad & k_1 = \kappa_1^{iv}, \ [\, k_2 = \kappa_2^{iv} + i\gamma, \ k_3 = \kappa_2^{iv}, \ k_4 = \kappa_2^{iv} - i\gamma \,], \\
(v): \quad & [\, k_1 = \kappa_1^v + i3\gamma/2, \ k_2 = \kappa_1^v + i\gamma/2, \ k_3 = \kappa_1^v - i\gamma/2, \ k_4 = \kappa_1^v - i3\gamma/2 \,],
\end{aligned}
$$

where all $\mathrm{Im}\,\{\kappa\} = 0$. Square brackets enclose bound-state strings. In any given string, adjacent quasi-momenta are separated in the complex direction by γ. The number of allowed configurations corresponds to the number of partitions of n photons into m bound states (where $2 \leqslant m \leqslant n$); the number of such partitions rapidly exceeds the number of particles.

In summary the previous few sections outline a procedure for obtaining a set of exact many-body eigenstates for the Dicke Hamiltonian, although no proof of their completeness has been given. This stumbling block will have to be addressed before it is possible to reliably extract scattering properties of the Hamiltonian from these interacting states.

2.3 Lippmann-Schwinger Scattering Theory

Given the set of exact eigenstates (2.25) it is then a nontrivial task to extract from them the many-body S-matrices. An obvious approach would be to appeal to the well established Lippmann-Schwinger scattering theory [40] that connects asymptotic incoming and outgoing states to fully interacting scattering orbits. This procedure is however not without certain subtleties and limitations [37, 41] which are the topic of this brief section which serves the additional purpose of introducing some general ideas that will be required later.

In scattering theory one frequently encounters Hamiltonians that naturally separate into two components, the first pertaining to the relevant free constituents; for example one can imagine a flux of inert itinerant particles incident on a fixed, local scatterer. The second component then accounts for any interactions between these two constituents, $\hat{H} = \hat{H}_0 + \hat{H}_{\text{int}}$. The state of the system in a scattering experiment develops according to $\hat{U}(t)|\psi\rangle$, where $\hat{U}(t) = e^{-i\hat{H}t}$ is the unitary fully-interacting time evolution operator. In practice incident few-particle states will be confined to wavepackets of finite duration and in the remote past, long before they reach the scatterer they essentially propagate freely according to the non-interacting time evolution operator, $\hat{U}^0(t) = e^{-i\hat{H}_0 t}$. This observation motivates the introduction of so-called in-states, defined in the following sense:

$$\left\| \hat{U}(t)|\psi\rangle - \hat{U}^0(t)|\psi_{in}\rangle \right\| \to 0 \quad \text{as} \quad t \to -\infty. \tag{2.27}$$

The two vectors, one a fully interacting orbit and the other a freely evolving incoming wavepacket, become increasingly indistinguishable in the remote past. Likewise once all the collision events are completed and the scattered particles have drifted far away from the scattering centre, the contribution of the interaction component of the Hamiltonian to the evolution of the state becomes insignificant; asymptotically free outgoing states, or out-states,

18

are then approached according to

$$\left|\left| \hat{U}(t) \left| \psi \right\rangle - \hat{U}^0(t) \left| \psi_{out} \right\rangle \right|\right| \to 0 \quad \text{as} \quad t \to \infty. \tag{2.28}$$

It does not necessarily follow that for every interacting orbit $\left| \psi \right\rangle$ there exist corresponding freely evolving incoming and outgoing states $\left| \psi_{in} \right\rangle$ and $\left| \psi_{out} \right\rangle$ according to (2.27) and (2.28). Such exceptions arise if, for example, $\hat{H}_{\text{int}}$ supports any bound states which remain forever confined to the interacting region.

The relation between these states and their corresponding interacting orbits are encoded in the so-called Møller wave operators; it follows from the definitions of the incoming and outgoing states given in (2.27) and (2.28) that

$$\left| i+ \right\rangle = \lim_{t \to -\infty} \hat{U}^+(t)\hat{U}^0(t) \left| i \right\rangle = \hat{\Omega}_+ \left| i \right\rangle, \tag{2.29}$$

that is, for each incoming state $\left| i \right\rangle$ the Møller operator $\hat{\Omega}_+$ provides a corresponding fully interacting state $\left| i+ \right\rangle$. Similarly for every outgoing state $\left| f \right\rangle$ there exists an actual scattering orbit $\left| f- \right\rangle$ whence it came that is generated by the Møller operator Ω_-

$$\left| f- \right\rangle = \lim_{t \to \infty} \hat{U}^+(t)\hat{U}^0(t) \left| f \right\rangle = \hat{\Omega}_- \left| f \right\rangle. \tag{2.30}$$

The possibility of bound states means that the Møller operators are not in general unitary. Nonetheless, it can be shown that every fully interacting orbit with an incoming state also has an outgoing state [42, 43], $\hat{\Omega}_+ \left| i \right\rangle = \left| i+ \right\rangle = \hat{\Omega}_- \left| f_i \right\rangle$ (where the subscript i in f_i is used to indicate its dependence on the initial state) and this property leads to the definition of a scattering matrix $\hat{S}$ which maps between them, $\left| f_i \right\rangle = \hat{\Omega}_-^+ \hat{\Omega}_+ \left| i \right\rangle = \hat{S} \left| i \right\rangle$. The bulk of scattering theory is concerned with calculating this matrix.

19

The probabilistic interpretation of the quantum wavefunction implies that real scattering states are both normalizable and non-stationary. The eigenstates of the non-interacting Hamiltonian, $\hat{H}_0 |p_n \ldots p_1\rangle = E(p_n \ldots p_1) |p_n \ldots p_1\rangle$ furnish a convenient orthonormal basis with which to expand incoming and outgoing states but when taken in isolation they satisfy neither of these requirements and consequently they are never approached in the limits (2.27) and (2.28). This problem is fixed by appreciating that since incoming/outgoing wavepackets come with their own internal distribution of momenta, applying the Møller operators to a proper state

$$\hat{\Omega}_\pm |\xi\rangle = \int d^n p \; \xi(p_n \ldots p_1) \; \hat{\Omega}_\pm |p_n \ldots p_1\rangle, \tag{2.31}$$

leads naturally to the introduction of the interacting basis vectors, $|p_n \ldots p_1 \pm\rangle = \hat{\Omega}_\pm |p_n \ldots p_1\rangle$. These vectors are eigenstates of the fully interacting Hamiltonian with the same energy as their non-interacting counterparts; that is, if $|p_n \ldots p_1\rangle$ is an eigenstate of $\hat{H}_0$ with energy E then $|p_n \ldots p_1 \pm\rangle$ will be eigenstates of $\hat{H}$ with the same energy.

In a theoretical investigation of a scattering problem one typically begins with a complete set of incoming plane waves $|p_n \ldots p_1\rangle$ that are defined in the remote past; these are then developed (in the context of a wavepacket) into fully interacting states expressible in terms of $|p_n \ldots p_1 +\rangle$ at time $t = 0$. Thes fully interacting orbits can be derived with the help of the following Lippmann-Schwinger relation which can be obtained from the definition of the retarded Møller operator (2.29):

$$|i+\rangle = |i\rangle + \hat{G}_0^R \hat{H}_{\text{int}} |i+\rangle \rightarrow |i+\rangle = \sum_{n=0}^{\infty} \left[\hat{G}_0^R \hat{H}_{\text{int}} \right]^n |i\rangle, \tag{2.32}$$

where $\hat{G}_0^R = (E - \hat{H}_0 + i0^+)^{-1}$ is the (free-particle) retarded Green's function. Once these interacting states are found a second Lippmann-Schwinger relation can be employed to determine their corresponding outgoing states

$$|f_i\rangle = |i+\rangle - \hat{G}_A^0 \hat{H}_{\text{int}} |i+\rangle, \tag{2.33}$$

which is derived from the definition of the advanced Møller operator (2.30). The advanced Green's function is defined as $\hat{G}_0^A = (E - \hat{H}_0 - i0^+)^{-1}$. Repeating this process for all possible incoming states yields all the information required to assemble a scattering matrix. The unitarity of this matrix clearly relies on the completeness of the incoming states.

In the unusual case that fully interacting states are already known, with the Bethe ansatz for example, then the corresponding incoming and outgoing states which are used to construct the scattering matrix can also be derived from the above Lippmann-Schwinger relations. However in contrast to the more conventional method (where the completeness of incoming states is guaranteed beforehand) a nontrivial completeness check on the resulting asymptotic states is now essential. This approach has already been followed by a group of authors [37] for one and two photons, although the complexity of the completeness check makes the scheme unsatisfactory.

More recently a conventional application of the Lippmann-Schwinger relations, beginning with a complete set of incoming plane waves has been used to calculate the fully interacting orbits developed for a one-dimensional channel of photons interacting with an an ensemble of n-level atoms [44].

2.4 Yudson-Rupasov Technique

2.4.1 Introduction and Derivation

Assuming that the complete set of eigenstates for the Hamiltonian (2.3) have been found then the time evolution of any given initial state ψ_n incorporating n-excitations can be determined by simply inserting a resolution of the identity in terms of them

$$|\psi_n(t)\rangle = e^{-i\hat{H}t} |\psi_n\rangle = \sum_{\text{allowed } k} e^{-iE_n t} |k_1, \ldots, k_n+\rangle \langle k_1, \ldots, k_n+|\psi_n\rangle. \qquad (2.34)$$

The allowed quasi-momenta appearing in (2.34) refer to a continuous spectrum of principal rapidities and a discrete set of complex configurations (2.26). This representation for the evolution is difficult to use; normalizing Bethe states is generally a formidable task [45] and the sum over configurations is tricky in practice. Fortunately a much more powerful and efficient procedure has been found that avoids such complications.

In the process of evaluating (2.34) with small numbers of particles Yudson and Rupasov discovered a 'latent simplicity'; cancellations between certain rapidity contributions occur predictably in each excitation subspace and this observation led them to a more refined representation for the time evolved state $\psi_n(t)$ in terms of an n-fold contour integral [22, 39]

$$|\psi_n(t)\rangle = \int_{\mathcal{C}_n} \frac{d^n\lambda}{(2\pi)^n} \, e^{-iE_\lambda^n t} \, |\lambda_1, \ldots, \lambda_n+\rangle \, (\bar{\lambda}_1, \ldots, \bar{\lambda}_n|\psi_n\rangle; \qquad (2.35)$$

the states $|\lambda_1, \ldots, \lambda_n+\rangle$ are the generalized eigenstates (2.25) with $N_n = 1$ and corresponding eigenenergies $E_\lambda^n = \lambda_1 + \lambda_2 + \cdots + \lambda_n$. The auxiliary states, distinguished by a rounded

parenthesis, are simply

$$|\lambda_1, \ldots, \lambda_n) = \int d^n x \, \theta \left(x_n < \cdots < x_1 \right) \prod_j f_{\lambda_j}(x_j) \, e^{i\lambda_j x_j} \, \hat{r}^+_{\lambda_j}(x_j) \, |\rangle. \qquad (2.36)$$

A key distinction between (2.34) and (2.35) is that the rapidities belonging to the latter are no longer restricted by periodicity. The contours of integration $\mathcal{C}_n$ depend on the particular choice of initial state; a typical scattering scenario for example finds a train of n photons impinging on an unexcited emitter:

$$|\psi_n\rangle = \hat{a}^+(x_n^0) \cdots \hat{a}^+(x_2^0)\hat{a}^+(x_1^0) \, |\rangle, \qquad x_n^0 < \cdots < x_2^0 < x_1^0 < 0. \qquad (2.37)$$

For such a configuration integration is performed over a series of contours parallel to the real axis; more precisely the contours are arranged such that $\mathcal{C} : \operatorname{Im}\{\lambda_{j+1}\} - \operatorname{Im}\{\lambda_j\} > \gamma$ for $j = 1, \ldots, n-1$ and $\operatorname{Im}\{\lambda_1\} > -\gamma/2$, as illustrated by figure 2.1.

The validity of the representation (2.35) will now be proved for the class of initial states (2.37). A general proof for arbitrary initial states can be found in the original paper [39]. Following the authors [22] this task is achieved in two stages. Firstly it is demonstrated that the representation faithfully returns the initial state at the initial instant, $t = 0$.

Due to the complementary ordering of the particle coordinates, the inner product between the initial and auxiliary state is $\langle \psi_n | \lambda_1, \ldots, \lambda_n) = \exp\left(i\lambda_1 x_1^0 + \cdots + i\lambda_n x_n^0 \right)$ and the right
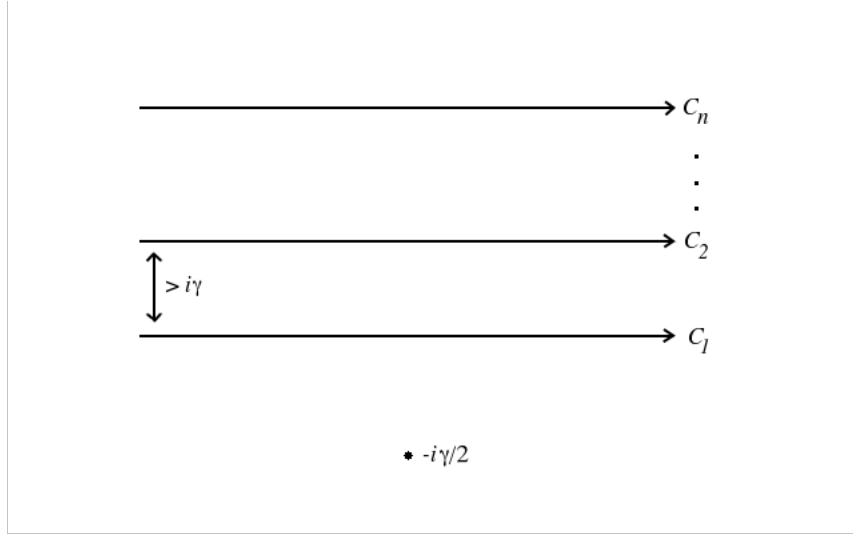
Figure 2.1: Contours of Integration for (2.35) with the initial state (2.37)

hand side of (2.35) at the initial instant becomes

$$\int d^n x \int_{\mathcal{C}_n} \frac{d^n \lambda}{(2\pi)^n} \prod_{i<j}\left[1 - \frac{2i\gamma\theta\left(x_i < x_j\right)}{\lambda_i - \lambda_j + i\gamma}\right] \prod_j f_{\lambda_j}\left(x_j\right) e^{i\lambda_j\left(x_j - x_j^0\right)} \left[\hat{a}^+\left(x_j\right) - \frac{\sqrt{\gamma}}{\lambda_j}\delta(x_j)\hat{S}^+\right] |\rangle.$$

(2.38)

Before proceeding to explicitly integrate (2.38) it is necessary to mention that when dealing with (2.35) one is often confronted with improperly defined integrals of the form

$$\int \frac{d\lambda}{2\pi} e^{i\lambda x} \varphi\left(\lambda\right)$$

(2.39)

with $\varphi\left(\lambda\right) \to 1$ as $|\lambda| \to \infty$, which have to be interpreted in the sense that

$$\int \frac{d\lambda}{2\pi} e^{i\lambda x} \varphi\left(\lambda\right) = \delta\left(x\right) - \int \frac{d\lambda}{2\pi} e^{i\lambda x}\left[\varphi\left(\lambda\right) - 1\right].$$

(2.40)

The contour integrals in (2.38) are calculated in the following way:

24

Calculating the contour integrals from the bottom up

- Supposing that $x_1 < x_1^0$ (< 0) then closing the contour $\mathcal{C}_1$ in the lower half plane incorporates no poles since the function $f_{\lambda_1}(x_1 < 0) = 1$ and the arrangement of the contours, in particular the fact that $\operatorname{Im}\{\lambda_1\} < \operatorname{Im}\{\lambda_{j>1}\} - \gamma$, prevents any instances where $\lambda_1 = \lambda_j - i\gamma$. Consequently $x_1 \geqslant x_1^0$ is essential if the representation (2.38) is to be non-zero.

- Likewise if $x_2 < x_2^0 < (x_1^0 \leqslant x_1)$ then the contour $\mathcal{C}_2$ can be completed in the lower half plane and the corresponding integral vanishes since the function $f_{\lambda_2}(x_2 < 0)$ is unity and $\theta(x_1 < x_2) = 0$ which eliminates any singularities that would have arisen when $\lambda_2 = \lambda_1 + i\gamma$. Therefore if any non-zero contributions exist then they are found exclusively in the regions $x_2 \geqslant x_2^0$ and $x_1 \geqslant x_1^0$.

Continuing with this line of reasoning leads to the requirement $x_j \geqslant x_j^0$ for all j.

Calculating the contour integrals from the top down

- Supposing that $x_n > x_n^0$ the contour $\mathcal{C}_n$ may be completed in the upper half plane without additional contribution. It follows by virtue of the ordering of the contours that the region bounded does not include any instances where $\lambda_n = \lambda_{i<n} + i\gamma$, nor does it incorporate the pole of the function $f_{\lambda_n}(x_n)$ at $\lambda_n = -i\gamma/2$. It is therefore necessary that $x_n \leqslant x_n^0$.

- Similarly, if $x_{n-1} > x_{n-1}^0$ then completing contour $\mathcal{C}_{n-1}$ in the upper half plane avoids the pole of the function $f_{\lambda_{n-1}}(x_{n-1})$. Moreover, since $x_n = x_n^0 < x_{n-1}^0 < x_{n-1}$ any divergences associated with $\lambda_{n-1} = \lambda_n - i\gamma$ are eliminated by $\theta(x_{n-1} > x_n) = 0$.

The above considerations reveal that any contributions to the contour integrals appearing in the representation (2.38) are restricted to the singular regions $x_j = x_j^0$ for all j, and are

25

proportional to $\delta\left(x_j - x_j^0\right)$. The result is a string of delta functions centred at the locations of the photons at the initial moment confirming the representation (2.38) at the initial instant for the class of states (2.37). In summary, the following observation has been made

$$|\psi_n\rangle = \int\limits_{\mathcal{C}_n} \frac{d^n\lambda}{(2\pi)^n} \; |\lambda_1, \ldots, \lambda_n+\rangle \left(\bar{\lambda}_1, \ldots, \bar{\lambda}_n \middle| \psi_n\right). \tag{2.41}$$

Since $|\lambda_1, \ldots, \lambda_n+\rangle$ are eigenstates of the Hamiltonian, the proof of the relation (2.35) for a train of incoming photons follows immediately by applying the time evolution operator to the left hand side of (2.41). The representation (2.35) for the evolution circumvents the subtle issue of completeness of the Bethe-states.

2.4.2 Single-Photon Scattering

Broadly two possibilities are open to a single photon incident on an unexcited atom: either the photon passes the emitter without interacting or it is absorbed and subsequently emitted after a delay $(\sim \gamma^{-1})$. Since it is impossible to determine which of these paths is taken without destroying coherence, both possibilities have to be accounted for at the level of the wavefunction which leads to some interesting interference with no classical explanation; such quantum interference effects will be the topic of subsequent sections. For a single photon beginning with a precise initial location, $x^0 < 0$, $t = 0$ the representation (2.35) predicts the following time-evolved photon state

$$\begin{aligned} G^1\left(x, \xi\right) &= \int\limits_{\mathcal{C}_1} \frac{d\lambda}{2\pi} \left[\theta(x < 0) + \frac{\lambda - i\gamma/2}{\lambda + i\gamma/2}\theta(0 < x)\right] e^{i\lambda(x-\xi)} \\ &= \delta\left(x - \xi\right) - \gamma\left(0 < x < \xi\right) e^{\gamma(x-\xi)/2}, \end{aligned} \tag{2.42}$$

where $\xi = x^0 + t$. The first contribution to the evolution represents unhindered propagation while the second term accounts for the radiation from the relaxation of the atomic excitation.

26

The scattered component is characterized by an exponential decay of amplitude to the left of the light cone. In practice a single incident photon can never be so well localized [46], but this presents no real difficulty since it is possible to expand any wavepacket in the basis of the elementary states that evolve according to (2.42).

Scattering matrices are typically given in the plane-wave basis; Fourier transforming (2.42) reveals that the important case of an incoming free-photon state

$$|i^1\rangle = \int dx \ h_k(x) \, \hat{a}^+(x) \, |\rangle, \tag{2.43}$$

where $h_k(x) = (2\pi)^{-1/2} e^{ikx}$ is scattered by the emitter into the outgoing free-photon state

$$|f_i^1\rangle = \int dx \ s_k h_k(x) \, \hat{a}^+(x) \, |\rangle, \tag{2.44}$$

which follows from (2.42) taken in the limit $t \to \infty$. The restriction $0 < x$ can be dropped since once a long time has elapsed one can be sure that the entirety of any incident wavepacket of finite duration will be found entirely to the right of scattering centre. An unimportant time dependent factor e^{-ikt} has been omitted in (2.44) and the scattering phase s_k is given in (2.7). With the results (2.43) and (2.44) a single photon S-matrix can be constructed, viz.

$$\hat{S}^1 = \sum_i |f_i^1\rangle\langle i^1| = \int dk \ s_k \, |k\rangle\langle k| \,. \tag{2.45}$$

In this case the unitarity of the scattering matrix is obvious.

2.4.3 Two-Photon Scattering

Much richer phenomena are to be expected for more than one incoming photon; the time evolution of a multi-photon state cannot simply be a product of the results for individual photon scattering since the finite spectrum of the emitter forbids double occupation. When two photons with the initial locations $x_2^0 < x_1^0 < 0$, $t = 0$ are incident on an initially unexcited emitter then the properly symmetrized photon wavefunction, $G_{sym}^2 (x_1 x_2, \xi_1 \xi_2)$ in the outgoing region $0 < x_1, x_2$ is readily obtained from (2.35), with the result

$$
\begin{aligned}
&\frac{1}{2!} \sum_Q \int_{\mathcal{C}_2} \frac{d^2\lambda}{(2\pi)^2} \left[1 - \frac{2i\gamma \, \theta \, (x_{Q_1} < x_{Q_2})}{\lambda_1 - \lambda_2 + i\gamma} \right] \prod_j \frac{\lambda_j - i\gamma/2}{\lambda_j + i\gamma/2} e^{i\lambda_j (x_{Q_j} - \xi_j)}, \\
&= \frac{1}{2!} \sum_Q \left[G^1 (x_{Q_1}, \xi_1) G^1 (x_{Q_2}, \xi_2) - 2\gamma^2 \theta \, (x_{Q_1} < x_{Q_2} < \xi_2 < \xi_1) \, e^{\gamma (x_{Q_1} + x_{Q_2} - \xi_2 - \xi_1)/2} \right],
\end{aligned} \tag{2.46}
$$

although it is slightly more physically insightful to write the state in the equivalent form

$$
G_{sym}^2 (x_2 x_1, \xi_1 \xi_2) = \sum_{Q'} \theta \left(x_{Q_2'} \leqslant \xi_2 \leqslant x_{Q_1'} \leqslant \xi_1 \right) \frac{1}{2!} \sum_Q G^1 (x_{Q_1}, \xi_1) G^1 (x_{Q_2}, \xi_2). \tag{2.47}
$$

The first term in the state (2.46) is representative of independent scattering while the second erases the possibility of finding two scattered photons in the regions $x_{Q_1} < x_{Q_2} < \xi_2 < \xi_1$. The structure of the two-photon wavefunction (2.46) is easy to interpret; since in free space photons do not disperse during propagation it is possible to trace their trajectories within each ordered sector. Double occupation of the atom is then implied if both of them, having been absorbed and subsequently emitted, are found to the left of the line $x = \xi_2$ as illustrated by the figure 2.2b. The impossibility of exciting the atom twice forbids such outcomes thereby restricting outgoing photons to the regions $x_{Q_2} \leqslant \xi_2 \leqslant x_{Q_1} \leqslant \xi_1$; otherwise they propagate freely which is evidenced by the equivalent representation (2.47). In other words, the ordering of jointly-scattered photons is prevented and this blockade-like effect is the essence of any induced photon correlations.

It follows from (2.46) that the incoming two-photon (plane wave) state

$$|i^2\rangle = \int d^2x \, \frac{1}{2!} \sum_Q h_{k_2}(x_{Q_2}) \, h_{k_1}(x_{Q_1}) \, \hat{a}^+(x_2) \, \hat{a}^+(x_1) \, |\rangle, \tag{2.48}$$

is scattered by the emitter into the outgoing state

$$|f_i^2\rangle = \int d^2x \, \frac{1}{2!} \left[\sum_Q s_{k_2} s_{k_1} h_{k_2}(x_{Q_2}) \, h_{k_1}(x_{Q_1}) \right.$$
$$\left. + \sum_{P,Q} B^2_{k_{P_2},k_{P_1}}(x_{Q_2}, x_{Q_1}) \right] \hat{a}^+(x_2) \, \hat{a}^+(x_1) \, |\rangle, \tag{2.49}$$

where the non-factorizable contribution in (2.46) amounts to a two-photon bound state

$$B^2_{k_2,k_1}(x_1, x_2) = -(s_{k_2} - 1)(s_{k_1} - 1) \, \theta(x_2 > x_1) \, h_{k_2}(x_2) h_{k_1}(x_2) \, e^{-\gamma|x_2 - x_1|/2}, \tag{2.50}$$

which can be attributed to the stimulated emission of the already excited emitter by the lagging photon. The state (2.50) derived from the Bethe ansatz is identical to the one obtained elsewhere by an alternative approach [36, 37, 47]. The two-photon S-matrix that follows from (2.48) and (2.49) is

$$\hat{S}^2 = \sum_i |f_i^2\rangle\langle i^2|$$
$$= \frac{1}{2!} \int d^2k \, s_{k_2} s_{k_1} |k_2, k_1\rangle\langle k_2, k_1| + \frac{1}{2!} \int d^4k \, B_{k'_2,k'_1,k_2,k_1} |k'_2, k'_1\rangle\langle k_2, k_1|, \tag{2.51}$$

where $B_{k'_2,k'_1,k_2,k_1} = 4 \, (\pi\gamma)^{-1} \, (t_{k'_2} + t_{k'_1}) t_{k_2} t_{k_1} \delta(k'_1 + k'_2 - k_1 - k_2)$ with $t_k = (s_k - 1)/2$ is the bound photon state (2.50) represented in momentum space. The first contribution to the scattering matrix preserves the photons' individual momenta and the second (inelastic) contribution redistributes momenta amongst the photons while conserving their total energy.
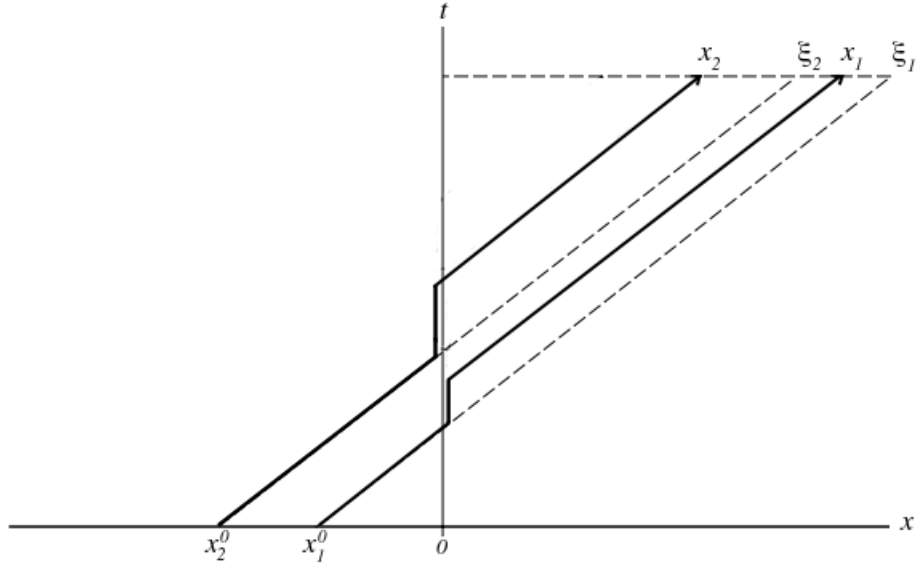
(a) Allowed path where both photons occupy the emitter.
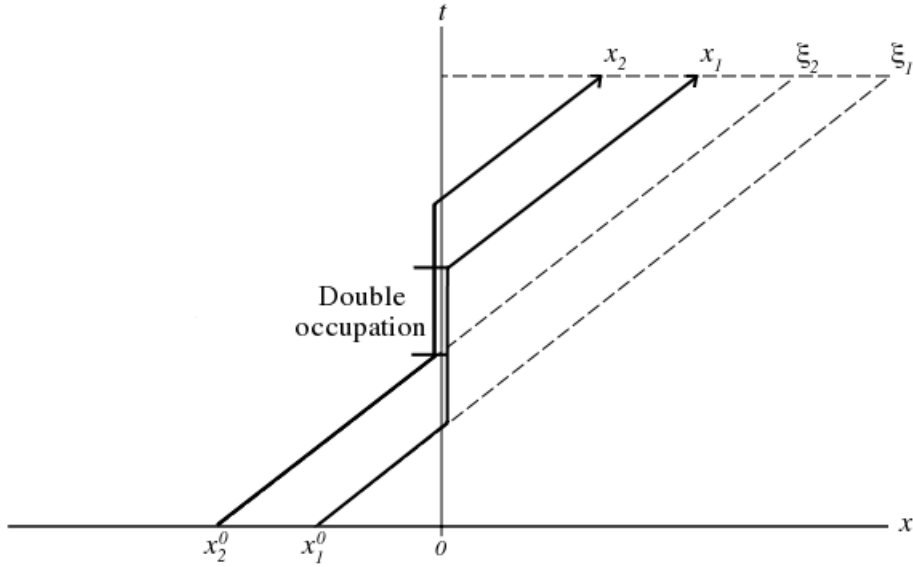
(b) Forbidden path since it requires double occupation of the emitter.

Figure 2.2: Within the ordered sector $x_2 < x_1$ the scattering channel that leaves both photons in the region $0 < x_2 < x_1 < \xi_2 < \xi_1$ is forbidden since it requires the two-level system to have been doubly occupied. A similar restriction exists for the alternative ordering $x_2 > x_1$ and follows directly from Bose symmetry.

2.4.4 Multi-Photon Scattering

The multi-photon scattered states that result from the interaction of photons with the emitter can be written in such a way as to yield a deeper insight into the essential physics at play in the dynamics of the Dicke model. The unsymmetrized outgoing wavefunction (2.35) that develops from a train of n incident photons (2.37) is

$$G^n(x_1 \ldots x_n, \xi_1 \ldots \xi_n) = \int_{\mathcal{C}_n} \frac{d^n \lambda}{(2\pi)^n} \prod_{i<j} \left[1 - \frac{2i\gamma\theta(x_i < x_j)}{\lambda_i - \lambda_j + i\gamma} \right] \prod_j \frac{\lambda_j - i\gamma/2}{\lambda_j + i\gamma/2} e^{i\lambda_j(x_j - \xi_j)}; \quad (2.52)$$

the physical photon wavefunction is of course symmetrized, that is

$$G^n_{sym}(x_1 \ldots x_n, \xi_1 \ldots \xi_n) = \frac{1}{n!} \sum_Q G^n(x_{Q_1} \ldots x_{Q_n}, \xi_1 \ldots \xi_n). \quad (2.53)$$

Considered in the particular ordered sector $x_n \leqslant x_{n-1} \leqslant \cdots \leqslant x_2 \leqslant x_1$ photons are restricted to the region $x_n \leqslant \xi_n \leqslant x_{n-1} \leqslant \cdots \leqslant \xi_2 \leqslant x_1 \leqslant \xi_1$ for precisely the same reasons as for the two-photon case, namely that any other possibility would require the emitter to have been doubly occupied, thus

$$\begin{aligned} G^n_{sym}&(x_n \leqslant \cdots \leqslant x_1, \xi_1 \ldots \xi_n) \\ &= \theta(x_n \leqslant \xi_n \leqslant \cdots \leqslant x_1 \leqslant \xi_1) \frac{1}{n!} \sum_Q G^n(x_{Q_1} \ldots x_{Q_n}, \xi_1 \ldots \xi_n). \end{aligned} \quad (2.54)$$

Since each $G^n(x_{Q_1} \ldots x_{Q_n}, \xi_1 \ldots \xi_n)$ vanishes outside the causal region, $x_{Q_j} \leqslant \xi_j$, $j = 1 \ldots n$ it can easily shown that the projection onto the permissible histories accounts for all of the correlation between photons. In other words the restriction of scattered photons to the region enforced by the global ordering in (2.54) renders the internal ordering, encoded by the theta

31

functions present in the square brackets in (2.52), superfluous [39] and consequently

$$
\begin{aligned}
G_{sym}^n &\left(x_n \leqslant \cdots \leqslant x_1, \xi_1 \ldots \xi_n \right) \\
&= \theta \left(x_n \leqslant \xi_n \leqslant \cdots \leqslant x_1 \leqslant \xi_1 \right) \frac{1}{n!} \sum_Q G^1 \left(x_{Q_n}, \xi_n \right) \cdots G^1 \left(x_{Q_1}, \xi_1 \right).
\end{aligned}
\tag{2.55}
$$

The full multi-photon wavefunction is then given by permuting over all sectors

$$
\begin{aligned}
G_{sym}^n &\left(x_n \ldots x_1, \xi_1 \ldots \xi_n \right) \\
&= \sum_Q \theta \left(x_{Q_n} \leqslant \xi_n \leqslant \cdots \leqslant x_{Q_1} \leqslant \xi_1 \right) \frac{1}{n!} \sum_{Q'} G^1 (x_{Q'_n}, \xi_n) \cdots G^1 (x_{Q'_1}, \xi_1).
\end{aligned}
\tag{2.56}
$$

Despite the physical clarity and compactness of this expression it is still awkward to use for calculating correlation functions and its representation in momentum space is untidy. For the purposes of the next few sections it will be more convenient to represent the scattered state in the equivalent form

$$
\begin{aligned}
G^n &\left(x_n \leqslant \cdots \leqslant x_1, \xi_1 \ldots \xi_n \right) \\
&= G^1 \left(x_n, \xi_n \right) \cdots G^1 \left(x_1, \xi_1 \right) - [\, \text{implied\ \ double\ \ occupation}\,],
\end{aligned}
\tag{2.57}
$$

and then to sum over symmetric permutations. Such representations arise naturally when the representation (2.52) is evaluated case by case, compare with (2.46). In this way it can be shown that the n-photon incoming plane waves

$$
i^n \left(x_1, x_2 \ldots x_n \right) = \frac{1}{n!} \sum_Q h_{k_n} \left(x_{Q_n} \right) \cdots h_{k_1} \left(x_{Q_1} \right),
\tag{2.58}
$$

are mapped by interaction onto the following outgoing states (for $n = 3, 4$)

$$
f_i^3 (x_1, x_2, x_3) = \frac{1}{3!} \left[\sum_Q s_{k_3} s_{k_2} s_{k_1} \, h_{k_3} (x_{Q_3}) \, h_{k_2} (x_{Q_2}) \, h_{k_1} (x_{Q_1}) \right.
$$
$$
\left. + \sum_{P,Q} s_{k_{P_3}} \, h_{k_{P_3}} (x_{Q_3}) \, B_{k_{P_2},k_{P_1}}^2 (x_{Q_2}, x_{Q_1}) + \sum_{P,Q} B_{k_{P_3},k_{P_2},k_{P_1}}^3 (x_{Q_3}, x_{Q_2}, x_{Q_1}) \right],
$$

(2.59)

$$
f_i^4 (x_1, x_2, x_3, x_4) = \frac{1}{4!} \left[\sum_Q s_{k_4} s_{k_3} s_{k_2} s_{k_1} \, h_{k_4} (x_{Q_4}) \, h_{k_3} (x_{Q_3}) \, h_{k_2} (x_{Q_2}) \, h_{k_1} (x_{Q_1}) \right.
$$
$$
+ \sum_{P,Q} s_{k_{P_4}} s_{k_{P_3}} \, h_{k_{P_4}} (x_{Q_4}) \, h_{k_{P_3}} (x_{Q_3}) \, B_{k_{P_2},k_{P_1}}^2 (x_{Q_2}, x_{Q_1})
$$
$$
+ \sum_{P,Q} B_{k_{P_4},k_{P_3}}^2 (x_{Q_4}, x_{Q_3}) \, B_{k_{P_2},k_{P_1}}^2 (x_{Q_2}, x_{Q_1}) + \sum_{P,Q} s_{k_{P_4}} \, h_{k_{P_4}} (x_{Q_4}) \, B_{k_{P_3},k_{P_2},k_{P_1}}^3 (x_{Q_3}, x_{Q_2}, x_{Q_1})
$$
$$
\left. + \sum_{P,Q} B_{k_{P_4},k_{P_3},k_{P_2},k_{P_1}}^4 (x_{Q_4}, x_{Q_3}, x_{Q_2}, x_{Q_1}) \right],
$$

(2.60)

where the n-photon bound states are

$$
B_{k_1,\ldots,k_n}^n (x_1, \ldots, x_n)
$$
$$
= -(-2)^{n-2} \prod_{i=1}^n (s_{k_i} - 1) \prod_{i=1}^{n-1} \theta (x_{i+1} > x_i) \, h_{k_{i+1}} (x_{i+1}) \, h_{k_1} (x_n) \, e^{-\gamma |x_n - x_1|/2}.
$$

(2.61)

There is a one-to-one correspondence between the terms in the four photon outgoing states of (2.60) and the allowed groups of complex rapidities (solutions of the Bethe-equations (2.26)). The extension to incident states with $n > 4$ photons is straightforward; the resulting states incorporate all possible partitions into bound states with any remaining photons written as products of single photon states. Each term will be reflected in the complex solutions of Bethe equations.

The outgoing states (2.59) and (2.60) are identical to those obtained in reference [47] that

are derived by explicitly solving the equations of motion (2.6) with open boundary conditions for each incoming photon number subspace. This further supports the conclusion that in the limit of large system size the particular choice of boundary conditions becomes irrelevant.

INCOMING STATE   OUTGOING STATES
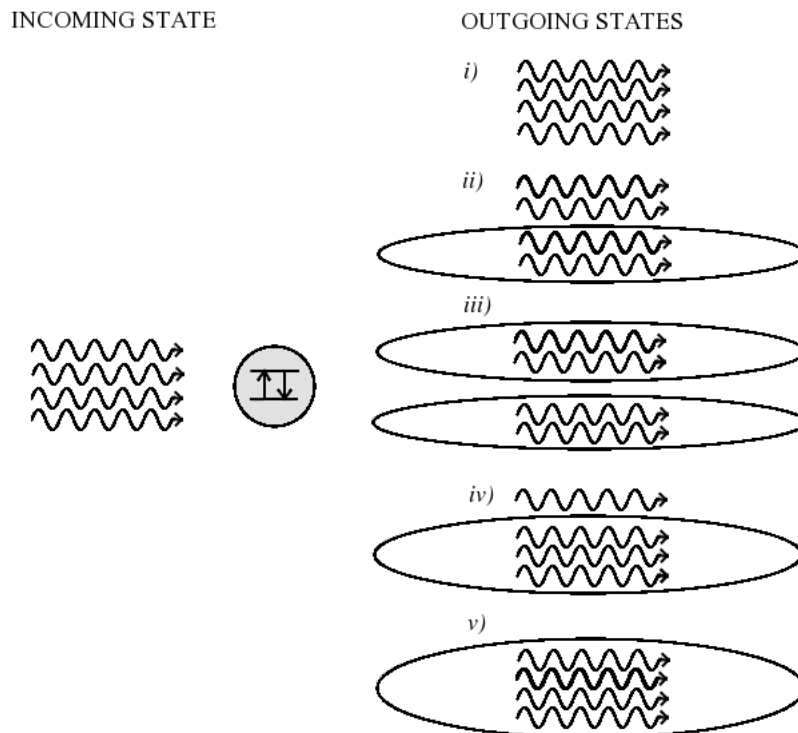
Figure 2.3: Depiction of the bound states created in the scattering of four quasi-resonant photons by a two-level impurity. There is a one-to-one correspondence between each of the possible outgoing states on the left and the quasi-momentum configurations permitted by the Bethe equations (2.26).

2.5 Scattering and the Quantum Langevin Equations

2.5.1 Derivation of the Quantum Langevin Equations

An alternative, more efficient derivation of the few-photon scattering matrices for the Dicke model has recently been found [48] by extending the standard input-output formalism of Gardiner and Collett [49] in the theory of damped quantum systems. Here the quantum Langevin equations for an arbitrary system linearly coupled to a bath of noninteracting bosons are derived. The standard input and output operators are introduced and their relation to the incoming and outgoing asymptotes of scattering theory is presented. The relevant Hamiltonian with which the input-output formalism is developed naturally divides into three terms:

$$\hat{H} = \hat{H}_{sys} + \int d\omega \; \omega \; \hat{b}_\omega^+ \hat{b}_\omega + \int d\omega \; \kappa_\omega \big(\hat{b}_\omega^+ \hat{c} + \hat{c}^+ \hat{b}_\omega \big). \tag{2.62}$$

The first is kept arbitrary and pertains to the system, while the second accounts for the bath of particles with corresponding creation and annihilation operators $\hat{b}_\omega^+$ and $\hat{b}_\omega$, which for any given mode do not commute, $\big[\hat{b}_\omega, \hat{b}_{\omega'}^+\big] = \delta(\omega - \omega')$. The interaction between this bosonic field and the system is then encoded in the final term where $\hat{c}$ is one of the possible system variables. For generality, the commutation relations between these variables which may be spin-like or bosonic are left unspecified at this point. The Heisenberg equations of motion for $\hat{b}_\omega$ and an arbitrary system operator $\hat{a}$ are

$$\dot{\hat{b}}_\omega = -i\omega \hat{b}_\omega - i\kappa_\omega \hat{c}, \qquad \dot{\hat{a}} = -i\big[\hat{a}, \hat{H}_{sys}\big] - i \int d\omega \; \kappa_\omega \big(\hat{b}_\omega^+ \big[\hat{a}, \hat{c}\big] + \big[\hat{a}, \hat{c}^+\big] \hat{b}_\omega \big). \tag{2.63}$$

Formally integrating the equation for $\hat{b}_\omega$ gives

$$\hat{b}_\omega(t) = e^{-i\omega(t-t_0)} \hat{b}_\omega(t_0) - i\kappa_\omega \int_{t_0}^{t} dt' \; e^{-i\omega(t-t')} \hat{c}(t'), \quad t_0 < t. \tag{2.64}$$

The first contribution, proportional to the initial value of the bath operator, is associated with the free evolution of the incident field, while second accounts for scattering from the system and spontaneous emission. Substituting (2.64) into the second relation in (2.63) generates the following representation for the evolution of $\hat{a}$ in terms of the incoming state of the field:

$$\dot{\hat{a}} = -i\left[\hat{a}, \hat{H}_{sys}\right] - i \int d\omega \, \kappa_\omega \left\{ e^{i\omega(t-t_0)} \hat{b}_\omega^+ (t_0) \left[\hat{a}, \hat{c}\right] + \left[\hat{a}, \hat{c}^+\right] e^{-i\omega(t-t_0)} \hat{b}_\omega (t_0) \right\}$$
$$+ \int d\omega \, \kappa_\omega^2 \int_{t_0}^{t} dt' \left\{ e^{i\omega(t-t')} \hat{c}^+ (t') \left[\hat{a}, \hat{c}\right] - \left[\hat{a}, \hat{c}^+\right] e^{-i\omega(t-t')} \hat{c} (t') \right\}, \tag{2.65}$$

where for compactness operators without time arguments are taken at time t.

Input Fields

In practice frequency integrals are taken over positive real values. However it is typical in optics for a shift to be made into a rotating frame defined by some frequency Ω characteristic of the the system; this alters the relevant frequency region to $\omega \in [-\Omega, \infty)$. When the frequency Ω is much greater than the interaction bandwidth the range of integration may be extended over the entire real line without introducing any significant error [50]. The relation (2.65) is exact; however a great simplification is afforded when the coupling is roughly independent of frequency, $\kappa_\omega = \sqrt{\gamma/2\pi}$ within the relevant range. Then the relations

$$\int_{-\infty}^{\infty} d\omega \, e^{i\omega(t-t')} = 2\pi\delta(t-t'), \qquad \int_{t_0}^{t} dt' \, \delta(t-t') \, \hat{c}(t') = \frac{1}{2}\hat{c}(t), \tag{2.66}$$

can be applied to (2.65), resulting in

$$\dot{\hat{a}} = -i\left[\hat{a}, \hat{H}_{sys}\right] - \left[\hat{a}, \hat{c}^+\right]\left(\frac{\gamma}{2}\hat{c} + \sqrt{\gamma}\,\hat{b}_{in}\right) + \left(\frac{\gamma}{2}\hat{c}^+ + \sqrt{\gamma}\,\hat{b}_{in}^+\right)\left[\hat{a}, \hat{c}\right], \tag{2.67}$$

where the input field is defined as

$$\hat{b}_{in}(t) = \frac{1}{\sqrt{2\pi}} \int d\omega \; e^{-i\omega(t-t_0)} \, \hat{b}_\omega(t_0), \tag{2.68}$$

with the commutation relations $\left[\hat{b}_{in}(t), \hat{b}_{in}^+(t')\right] = \delta(t - t')$. The expression (2.67) is the quantum equivalent of a Langevin equation for the variable $\hat{a}$, with $\hat{b}_{in}(t)$ and $\hat{b}_{in}^+(t)$ replacing classical noise terms. The consequence of having assumed a frequency independent coupling is that the evolution of $\hat{a}$ follows independently of its history. This lack of memory is rarely exact and is referred to as a Markov approximation.

Output Fields

A time-reversed version of the quantum Langevin equations can be found by representing the bath operators in the following somewhat unnatural form, with their present state expressed in terms of their future motion

$$\hat{b}_\omega(t) = e^{-i\omega(t-t_1)}\hat{b}_\omega(t_1) + i\kappa_\omega \int_t^{t_1} dt' \; e^{-i\omega(t-t')}\hat{c}(t'), \quad t < t_1. \tag{2.69}$$

Substituted into (2.65) it generates

$$\dot{\hat{a}} = -i\left[\hat{a}, \hat{H}_{sys}\right] - \left[\hat{a}, \hat{c}^+\right]\left(-\frac{\gamma}{2}\hat{c} + \sqrt{\gamma}\,\hat{b}_{out}\right) + \left(-\frac{\gamma}{2}\hat{c}^+ + \sqrt{\gamma}\,\hat{b}_{out}^+\right)\left[\hat{a}, \hat{c}\right], \tag{2.70}$$

with the output field is defined as

$$\hat{b}_{out}(t) = \frac{1}{\sqrt{2\pi}} \int d\omega \; e^{-i\omega(t-t_1)} \, \hat{b}_\omega(t_1). \tag{2.71}$$

Input-Output Formula

A relation between the input and output fields can be obtained by integrating (2.64) and (2.69) over all frequencies, that is

$$\hat{b}_{in}(t) - i\frac{\sqrt{\gamma}}{2}\hat{c}(t) = \int d\omega\, \hat{b}_\omega(t) = \hat{b}_{out}(t) + i\frac{\sqrt{\gamma}}{2}\hat{c}(t). \tag{2.72}$$

This relation is the basis of the scattering theory developed in the next section.

2.5.2 Application to Scattering Theory

Identification of the input and output operators of the quantum Langevin formalism with the incoming and outgoing asymptotes of scattering theory can be exploited to provide the S-matrices for a variety of scattering problems [48] although further approximations than previously discussed are typically necessary. In the specific case of the Dicke model the system operators $\hat{c}$ and $\hat{c}^+$ in (2.62) are replaced with the atomic psuedo-spin operators $\hat{S}^-$ and $\hat{S}^+$ respectively and the bosonic bath operators correspond to the photon annihilation and creation operators, $\hat{b}_\omega \to \hat{a}_k$ and $\hat{b}_\omega^+ \to \hat{a}_k^+$. The Møller operators defined in (2.29) and (2.30) facilitate a representation of scattering matrix elements in the basis of non-interacting n-photon plane-wave states

$$S^n_{k'_n,\dots k'_1, k_n,\dots k_1} = \langle k'_n, \dots k'_1 | \hat{\Omega}^+_- \hat{\Omega}_+ | k_n, \dots k_1 \rangle. \tag{2.73}$$

Reference to the emitter has been suppressed since initially it is assumed to be unexcited and once interactions are over it returns to its ground state via spontaneous emission; the scatterer therefore has only intermediary significance, matching asymptotically free incoming states to outgoing ones. It is helpful to define incoming and outgoing scattering operators

respectively as

$$\hat{A}_k^+ = \hat{\Omega}_+ \hat{a}_k^+ \hat{\Omega}_+^+, \qquad \hat{B}_k^+ = \hat{\Omega}_- \hat{a}_k^+ \hat{\Omega}_-^+, \tag{2.74}$$

which are constructed so as to generate fully interacting eigenstates from vacuum, that is $\hat{A}_{k_n}^+ \cdots \hat{A}_{k_1}^+ |\rangle = |k_n \ldots k_1+\rangle$ and $\hat{B}_{k_n}^+ \cdots \hat{B}_{k_1}^+ |\rangle = |k_n \ldots k_1-\rangle$. The interacting eigenstates $|k_n \ldots k_1+\rangle$ are those that develop from the plane-waves $|k_n \ldots k_1\rangle$ while it is in the context of a wavepacket of finite duration (2.31). In a similar sense, $|k_n \ldots k_1-\rangle$ are the interacting eigenstates that asymptotically approach the non-interacting plane-waves $|k_n \ldots k_1\rangle$ once all photons have passed through the interacting region. It follows from the unitarity of the Møller transformation for the Dicke model (this will be proved later) that the scattering operators conform to the commutation relations $[\hat{A}_k, \hat{A}_{k'}^+] = \delta(k - k')$, $[\hat{B}_k, \hat{B}_{k'}^+] = \delta(k - k')$. In terms of these operators the scattering matrix elements have the succinct representation

$$S_{k_n',\ldots k_1',k_n,\ldots k_1}^n = \langle| \hat{B}_{k_n'} \cdots \hat{B}_{k_1'} \hat{A}_{k_n}^+ \cdots \hat{A}_{k_1}^+ |\rangle. \tag{2.75}$$

Expressed in the time domain, $\hat{A}_k^+$ and $\hat{B}_k^+$ are simply the input and output operators that were defined in (2.68) and (2.71), viz.

$$\hat{a}_{in}(t) = \frac{1}{\sqrt{2\pi}} \int dk \, e^{-ik(t-t_0)} \hat{a}_k(t_0) = \frac{1}{\sqrt{2\pi}} \int dk \, e^{-ikt} e^{-i\hat{H}t_0} e^{-i\hat{H}_0 t_0} \hat{a}_k e^{i\hat{H}_0 t_0} e^{-i\hat{H}t_0},$$
$$\to \frac{1}{\sqrt{2\pi}} \int dk \, e^{-ikt} \hat{\Omega}_+ \hat{a}_k^+ \hat{\Omega}_+^+ = \hat{A}(t), \quad t_0 \to -\infty. \tag{2.76}$$

Similarly it can be shown that $\hat{a}_{out}(t) \to \hat{B}(t)$ in the limit $t_1 \to \infty$ establishing a useful connection between scattering theory and the quantum Langevin equations.

The results of the input-output formalism, principally the relations (2.67) and (2.72), provide an efficient scheme for calculating the few-photon scattering matrices (2.73) [48]. It will be

useful for subsequent analysis to rewrite the input-output formula (2.72) in momentum space

$$\hat{B}_k = \hat{A}_k - i\sqrt{\frac{\gamma}{2\pi}} \int dt\, e^{ikt}\, \hat{S}^-(t). \tag{2.77}$$

Single-Photon S-matrix

A consequence of the relation (2.77) is that single-photon scattering matrix elements may be written in the form

$$S^1_{k',k} = \langle| \hat{B}_{k'} \hat{A}^+_k |\rangle = \delta(k - k') - i\sqrt{\frac{\gamma}{2\pi}} \int dt\, e^{ik't}\, \langle| \hat{S}^-(t)\, |k+\rangle, \tag{2.78}$$

with an obvious physical significance: the state of an incoming photon remains unchanged unless at sometime during the interaction window the emitter is engaged. The amplitude for finding the atom occupied in the fully interacting state is calculated from the Langevin equation (2.67) for the atomic pseudo-spin operator $\hat{S}^-$, that is

$$\begin{aligned}
\langle| \dot{\hat{S}}^-(t)\, |k+\rangle &= 2i\sqrt{\gamma}\, \langle| \hat{S}^z(t)\hat{a}_{in}(t)\, |k+\rangle - \frac{\gamma}{2} \langle| S^-(t)\, |k+\rangle \\
&= -i\sqrt{\frac{\gamma}{2\pi}}e^{-ikt} - \frac{\gamma}{2} \langle| S^-(t)\, |k+\rangle,
\end{aligned} \tag{2.79}$$

where the final expression follows from the relation $\hat{S}^z(t)\,|\rangle = -1/2$. The solution to the equation (2.79) that is bounded as $t \to \infty$ is

$$\langle| \hat{S}^+(t)\, |k+\rangle = \sqrt{\frac{\gamma}{2\pi}} \frac{e^{-ikt}}{k + i\gamma/2}, \tag{2.80}$$

which when substituted into (2.78) returns the following single photon scattering matrix elements confirming the Yudson-Rupasov result (2.45):

$$S^1_{k',k} = s_{k'}\delta(k' - k), \qquad s_k = \frac{k - i\gamma/2}{k + i\gamma/2}, \tag{2.81}$$

40

Two-Photon S-Matrix

The simplest route to the two-photon scattering matrix is achieved by inserting a resolution of unity in terms of the interacting single excitation states

$$S^2_{k'_2,k'_1,k_2,k_1} = \langle| \hat{B}_{k'_2}\hat{B}_{k'_1}\hat{A}^+_{k_2}\hat{A}^+_{k_1} |\rangle = \langle k'_2-| \int dp \ |p+\rangle\langle p+| \hat{B}_{k'_1} |k_2, k_1+\rangle. \qquad (2.82)$$

Since $\langle k'_2 - |p+\rangle = \langle| \hat{B}_{k'_2}\hat{A}^+_p |\rangle$ is simply the single-photon scattering matrix element (2.81) the expression (2.82) reduces to

$$S^2_{k'_2,k'_1,k_2,k_1} = s_{k'_2} \langle k'_2+| \hat{B}_{k'_1} |k_2, k_1+\rangle. \qquad (2.83)$$

The relation between incoming and outgoing scattering operators (2.77) can now be applied effectively

$$\langle k'_2+| \hat{B}_{k'_1} |k_2, k_1+\rangle = \sum_P \delta(k'_2 - k_{P_2})\delta(k'_1 - k_{P_1}) - i\sqrt{\frac{\gamma}{2\pi}} \int dt \ e^{ik'_1 t} \ \langle k'_2+| \hat{S}^-(t) |k_2, k_1+\rangle.$$

$$(2.84)$$

A naive substitution of both $\hat{B}_k$ operators in (2.82) using the input-output formula without having first substituted the resolution of the identity would have led to two-time averages, $\langle| \hat{S}^-(t')\hat{S}^-(t) |k_2, k_1+\rangle$ that are difficult to deal with exactly. The excitation amplitude $\langle k'_2+| \hat{S}^-(t) |k_2, k_1+\rangle$ in (2.84) is found by appealing to the the Langevin equation for $\hat{S}^-$ which in the current context gives

$$\langle k'_2+| \dot{\hat{S}}^-(t) |k_2, k_1+\rangle = 2i\sqrt{\frac{\gamma}{2\pi}} \sum_P \langle k'_2+| \hat{S}^z(t) |k_{P_2}+\rangle e^{-ik_{P_1}t} - \frac{\gamma}{2} \langle k'_2+| S^-(t) |k_2, k_1+\rangle.$$

$$(2.85)$$

The first term is simplified by employing the relation $\hat{S}^z(t) = \hat{S}^+(t)\hat{S}^-(t) - 1/2$ and noting that since there is only one emitter and the number of excitations is conserved during time

evolution, then

$$\langle k'+|\, \hat{S}^+(t)\hat{S}^-(t)\,|k+\rangle \,=\, \langle k'+|\, \hat{S}^+(t)\,|\rangle\langle|\, \hat{S}^-(t)\,|k+\rangle \,=\, \frac{\gamma}{2\pi}\frac{e^{ik't}}{k'-i\gamma/2}\frac{e^{-ikt}}{k+i\gamma/2}, \qquad (2.86)$$

which follows from the relation (2.80). The above result completes the equation (2.85) for the spin amplitude; the relevant solution is

$$\begin{aligned}\langle k_2'+|\, \hat{S}^-(t)\,|k_2,k_1+\rangle =&\sqrt{\frac{\gamma}{2\pi}}\sum_P \frac{e^{-ik_{P_1}t}}{k_{P_1}+i\gamma/2}\delta(k_2'-k_{P_2})\\ &+\frac{8i}{\pi\gamma^2}\sqrt{\frac{\gamma}{2\pi}}\,\bar{t}_{k_2'}t_{k_2+k_1-k_2'}(t_{k_2}+t_{k_1})e^{-i(k_2+k_1-k_2')t},\end{aligned} \qquad (2.87)$$

where $t_k = (s_k - 1)/2$. Relations (2.87), (2.84) and (2.83) combine to provide the scattering matrix elements [48]

$$S^2_{k_2',k_1',k_2,k_1} = \sum_P s_{k_2}s_{k_1}\delta(k_2'-k_{P_2})\delta(k_1'-k_{P_1}) + \frac{8}{\pi\gamma}t_{k_2'}t_{k_1'}(t_{k_2}+t_{k_1})\delta(k_2'+k_1'-k_2-k_1),$$

$$(2.88)$$

which are equivalent to those obtained by the Yudson-Rupasov (YR) technique (2.51). In principle one could continue to use the input-output formula to determine S-matrix elements for arbitrarily many photons, but the calculations required become increasingly cumbersome and eventually it becomes much more straightforward to resort to the YR technique. The key advantage of this scheme is its scope of applicability and its efficiency: it is readily adapted to deal with other scattering problems and avoids any explicit representations of the fully interacting many-body eigenstates of the Hamiltonian. Despite its efficiency and generality, the underlying physics elucidated by the YR approach is much less transparent.

CHAPTER 3

QUANTUM OPTICAL COHERENCE

3.1 Introduction

It was observations concerning light and not matter that launched us into the quantum era with Planck's realization that the absurd classical prediction concerning diverging radiation intensities at short wavelengths for a blackbody is averted if the the amounts by which the electromagnetic field can exchange energy with matter are quantized. Einstein developed this idea further: with a minimum of assumptions he derived the entropy of this radiation and observed its similarity to that of a gas of identical particles [51]. This photon paradigm offered a powerful conceptual tool accounting for the then recently discovered photo-electric effect and Compton scattering, and it is now indispensable in the field of quantum optics.

Given the history it is then perhaps surprising that a complete quantum theory of light took much longer to get established than its condensed matter counterpart. This is due in no small part to the absence of an unambiguous definition for the photon position operator [46], a stumbling block eventually sidestepped in the mid 1960s when Glauber devised a quantum description of optical coherence that closely resembles classical theory [52]. Central to this theory is the concept of an ideal photon detector that absorbs and registers incident photons.

In a typical interference experiment light from several sources is mixed and field correlations are then measured between various locations and times. Optical coherence is characterized by the dependence of these correlations on optical path length, phase shifts and/or times of measurement. This chapter categorizes a few relevant types of interference, highlighting some essential quantum aspects. Photon bunching and anti-bunching is briefly discussed in preparation for later sections and the classic Hong-Ou-Mandel experiment is introduced [23], a landmark in quantum optics illustrating a quintessentially quantum interference effect. In this experiment two photons arriving simultaneously at a lossless balanced beamsplitter from distinct incoming ports are always found exiting together in one of the two possible outgoing ports. This coalescence is associated with the indistinguishability of the photons and the resulting interference of Feynman paths. The final section determines the extent to which the nonlinearity introduced by a single two-level atom operating as a beamsplitter alters this phenomena.

3.2   Single-Photon Interference

Single-photon interference refers to two-point correlations of the electric field exhibited in both Young's and Michelson's interferometry. All classical interference is of this type and it will be shown that at this level interference between different photons can not be inferred. Instead all observations are explained with the assumption that each photon interferes only with itself [53], a principle that fails to properly account for some aspects of higher order coherence. Before introducing the theory of Glauber it is appropriate to define what is meant by an ideal photon detector. A detailed theory of photo-detection is well established in the literature (a thorough review can be found in [54] and citations contained therein). For the purposes of the following sections it is sufficient to provide a brief heuristic analysis.

In vacuum the quantum electric and magnetic field operators satisfy a quantized version of Maxwell's equations and separate naturally into contributions from positive and negative frequencies, for example

$$\hat{\mathbf{E}}\left(\mathbf{r}, t\right) = i \sum_k \sqrt{\frac{\hbar \omega_k}{2 \varepsilon_0}} \mathbf{u}_k(\mathbf{r}) e^{-i \omega_k t} \hat{a}_k^+ + \text{h.c.} = \hat{\mathbf{E}}^{(-)}\left(\mathbf{r}, t\right) + \hat{\mathbf{E}}^{(+)}\left(\mathbf{r}, t\right); \qquad (3.1)$$

the vectors $\mathbf{u}_k(\mathbf{r})$ are transverse orthonormal mode functions. In free space they satisfy, $\nabla^2 \mathbf{u}_k - (\omega_k^2/c^2)\mathbf{u}_k = 0$, supplemented by the appropriate boundary conditions. The resulting modes are indexed by k which may refer to several distinct variables (discrete or continuous) such as polarization and momentum. When the field is confined to a cube with side length L the relevant modes are $\mathbf{u}_k(\mathbf{r}) = L^{-3/2}\hat{\mathbf{e}}_{\mathbf{k},\mu}e^{i\mathbf{k}\cdot\mathbf{r}}$ where the field polarization is encoded in the unit vectors $\hat{\mathbf{e}}_{\mathbf{k},\mu}$; the transversality requirement means that $\hat{\mathbf{e}}_{\mathbf{k},\mu} \cdot \mathbf{k} = 0$. For the quantized field the positive and negative frequency components $\hat{\mathbf{E}}^{(-)}\left(\mathbf{r}, t\right)$ and $\hat{\mathbf{E}}^{(+)}\left(\mathbf{r}, t\right)$ take on the role of real space creation and annihilation operators [55] respectively. The essential property of the quantum field distinguishing it from its classical counterpart is that the positive and negative frequency components taken at different time-like separated regions do not generally commute, in particular the operators $\hat{a}_k$ and $\hat{a}_k^+$ can be shown to exhibit Bose commutation relations. In the interaction and Heisenberg pictures the interaction of light field with matter gets encoded in the time development of these operators.

A wide variety of techniques have now been developed that are capable of detecting light with single-photon resolution, including some quantum non-demolition schemes that employ highly sensitive Kerr nonlinearities to achieve single photon detection while leaving the state of the detected photon intact [56]. The majority of measurements however are absorptive and rely on some variant of the photo-electric effect. Electrons bound to a photoemissive surface are exposed to incident light; a single incoming photon with energy above a certain

threshold is then likely to be absorbed by an electron, imparting sufficient energy for it to escape. Liberated electrons can then be amplified by electrical means into a detectable current (photo-count). It can be shown that once the typical incident photon frequencies are great enough such a detector will be sensitive to two-point correlations of the electric field. For polarized quasi-monochromatic incident light the probability that a photo-count is registered by a detector at $\mathbf{r}$, t within some short time interval Δt is proportional to the light intensity

$$p_1\left(\mathbf{r}, t\right)\Delta t = \eta \Delta t\left\langle \hat{I}\left(\mathbf{r}, t\right)\right\rangle, \tag{3.2}$$

where $\hat{I}\left(\mathbf{r}, t\right) = \hat{E}^-\left(\mathbf{r}, t\right)\hat{E}^+\left(\mathbf{r}, t\right)$ and $\eta = \alpha S c$, where α is the dimensionless detector efficiency and S is the area of the absorbing surface [54]. The intensity, $\left\langle \hat{I}\left(\mathbf{r}, t\right)\right\rangle = \Gamma_{\mu,\mu}^{(1,1)}\left(\mathbf{r}, t; \mathbf{r}, t\right)$ belongs to a much wider class of single-photon coherence functions

$$\Gamma_{\mu',\mu}^{(1,1)}\left(\mathbf{r}', t'; \mathbf{r}, t\right) = \mathrm{Tr}\left\{\hat{\rho}\,\hat{E}_{\mu'}^{(-)}\left(\mathbf{r}', t'\right)\hat{E}_{\mu}^{(+)}\left(\mathbf{r}, t\right)\right\}, \tag{3.3}$$

where the density matrix $\hat{\rho}$ describes the state of the light field before detection and μ and μ' are polarization indices. Interference that may be present in observables of the type (3.3) offers no information about any correlations that may or may not exist between photons. This point is relevant for later sections of this thesis and can be easily demonstrated in the context of Young's double slit interference experiment where polarized monochromatic light is channelled through two pinholes where their separation is much grater than their diameter (so that the diffraction pattern from individual pinholes can be reasonably ignored). The field at the detector is then the sum of two spherical waves

$$\begin{aligned}\hat{E}^{(+)}\left(\mathbf{r}, t\right) &= \hat{E}_1^{(+)}\left(\mathbf{r}, t\right) + \hat{E}_2^{(+)}\left(\mathbf{r}, t\right)\\ &= i\sqrt{\frac{\hbar\omega_k}{2\varepsilon_0}}u_{k,1}\left(\mathbf{r}\right)\hat{a}_1 e^{-i\omega_k t} + i\sqrt{\frac{\hbar\omega_k}{2\varepsilon_0}}u_{k,2}\left(\mathbf{r}\right)\hat{a}_2 e^{-i\omega_k t},\end{aligned} \tag{3.4}$$

46

the mode functions are

$$u_{k,j}\left(\mathbf{r}\right) = \frac{1}{\sqrt{2\pi R}} \frac{e^{ik|\mathbf{r}-\mathbf{r}_j|}}{|\mathbf{r}-\mathbf{r}_j|},$$ (3.5)

where R is the radius of the normalization volume. The annihilation operators $\hat{a}_1$ and $\hat{a}_2$ are associated with the radial modes of the field for photons arriving from the pinholes located at $\mathbf{r}_1$ and $\mathbf{r}_2$ respectively. If the distance from the pinholes to the detector is much greater the pinhole separation, then $|\mathbf{r}-\mathbf{r}_j|$ may be replaced by $|\mathbf{r}|$ in the denominator of (3.5) and the average intensity recorded by a detector located at $\mathbf{r}$ is found to be

$$\langle\hat{I}\left(\mathbf{r}\right)\rangle = |f\left(\mathbf{r}\right)|^2\left[\langle\hat{a}_1^+\hat{a}_1\rangle + \langle\hat{a}_2^+\hat{a}_2\rangle + 2\left|\langle\hat{a}_1^+\hat{a}_2\rangle\right|\cos\phi(\mathbf{r})\right].$$ (3.6)

where $f\left(\mathbf{r}\right)$ follows from the foregoing discussion. The cross term, responsible for interference, is generally complex, $\langle\hat{a}_1^+\hat{a}_2\rangle = \left|\langle\hat{a}_1^+\hat{a}_2\rangle\right|e^{i\delta}$, and contributes to a phase shift between photon paths $\phi(\mathbf{r}) = k\left|\mathbf{r}-\mathbf{r}_2\right| - k\left|\mathbf{r}-\mathbf{r}_1\right| + \delta$. The degree of first order mutual coherence between the light arriving from each slit is captured by the normalized correlation ratio

$$\left|\gamma_{1,2}^{(1,1)}\right| = \frac{\left|\langle\hat{a}_1^+\hat{a}_2\rangle\right|}{\sqrt{\langle\hat{a}_1^+\hat{a}_1\rangle\langle\hat{a}_2^+\hat{a}_2\rangle}},$$ (3.7)

which lies between 0 and 1 and is directly related to the degree of path indistinguishability [57]. In instances where it is possible, even if only in principle, to determine which of the two pinholes each photon arriving at the detector passed through then interference will not be observed, irrespective of whether this which-path information is actually gathered [58]. For example no interference of the type (3.6) will be observed for the fock state $|1_1, 0_2\rangle$ where a single photon is somehow known to have arrived at the detector from slit 1. In contrast interference is often exhibited where which-path information can not be determined or is only partial. In such cases it is natural to make a shift to modes with even and odd parity,

$\hat{a}_\pm = (\hat{a}_1 \pm \hat{a}_2)/\sqrt{2}$. The optimally indistinguishable single-photon state

$$|1_+, 0_-\rangle = \frac{1}{\sqrt{2}}\left[\, |1_1, 0_2\rangle + |0_1, 1_2\rangle \,\right], \tag{3.8}$$

has $\left|\gamma_{1,2}^{(1,1)}\right| = 1$ and generates an interference pattern with maximum fringe visibility

$$\langle \hat{I}_1(\mathbf{r})\rangle = |f(\mathbf{r})|^2 \left[\, 1 + \cos \phi(\mathbf{r}) \,\right]. \tag{3.9}$$

The mutual exclusivity of interference and which-path information is generally referred to as the complementarity principle. Interference is lost even when which-path knowledge is gained without ever directly probing the state of the light in the interferometer, in other words it is not simply that there is no device so sensitive as to detect the paths of each photon without disturbing them, but rather that complementarity is a fundamental aspect of reality. This point is perhaps best demonstrated by the fascinating experiment of Zou, Wang and Mandel with two-photon sources [59] depicted in figure 3.2.

The mode (3.8) shared by n-photons $|n_+, 0_-\rangle$ produces an intensity $\langle \hat{I}_n(\mathbf{r})\rangle = n\langle \hat{I}_1(\mathbf{r})\rangle$ which appears to suggest that each photon interferes only with itself although it will soon be clear that this assumption is false. A very different configuration of the field is generated by a single-mode laser operating above threshold which for short times is well approximated by the coherent state

$$|\alpha\rangle = e^{-|\alpha|^2/2} \sum_n \frac{\alpha^n}{\sqrt{n!}} |n\rangle. \tag{3.10}$$

The number of photons represented by the state (3.10) is poisson distributed, $p_n = \alpha^{2n} e^{-|\alpha|^2}/n!$ with mean photon number $\langle n\rangle = |\alpha|^2$. If such a state is incident on the two pinholes in equal proportion, for example via the indistinguishable mode $|\alpha_+, 0_-\rangle$ then the intensity at the detector will be $\langle \hat{I}_\alpha(\mathbf{r})\rangle = |\alpha|^2 \langle \hat{I}_1(\mathbf{r})\rangle$. Consequently, a Fock state containing precisely n

photons and a coherent state that only on average contains n photons (that is, $|\alpha| = n$) cannot be distinguished by appealing to first order correlations alone. It is generally true that the information gathered by an average of single detections is "insufficient to distinguish between states with identical spectra but differing photon number distributions" [60].

3.3 Multi-Photon Interference

Semi-classical theories, where matter is quantized and the radiation field is treated classically, have received a great deal of success describing non-classical optical phenomena. In order to expose the quantum nature of light one has to work hard to ensure that measurements made truly reflect the character of the field rather than merely being an artifact of the particular way in which radiation interacts with a detector. In practice this means that detections at multiple times and locations have to be taken in any given realization of an experiment; certain correlations between them can then be representative of the field only.

One of the simplest such experiments able to discriminate between the semi-classical and quantum descriptions of light was performed by Grangier, Roger and Aspect in 1974 [61]. In this experiment single photons are sent through a balanced beam splitter with detectors stationed at both exit ports (i.e a single photon is sent along arm 1 of the interferometer depicted in figure 3.1a for example, while the arm 2 remains empty). A two-photon source is chosen, such as an atomic cascade or parametric converter, and a third 'trigger' detector is placed near to the source so as to detect one photon from the pair thereby heralding the arrival of the other, which is then directed through the beam splitter towards one of the exit detectors, D_3 or D_4. The experiment reveals that a detection at the trigger is accompanied by a detection at only one of the exit detectors; triggering of both exit detectors never occurs. The result confirms the existence and indivisibility of single photons.
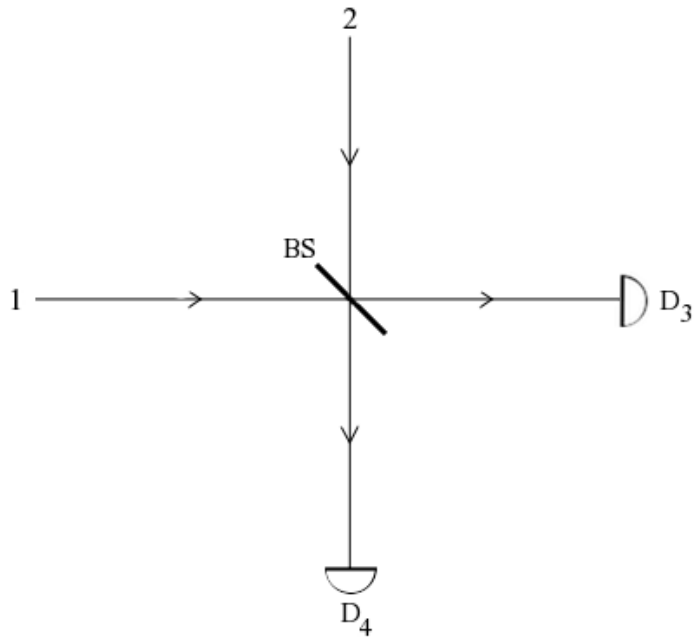
(a) A typical beamsplitter arrangement
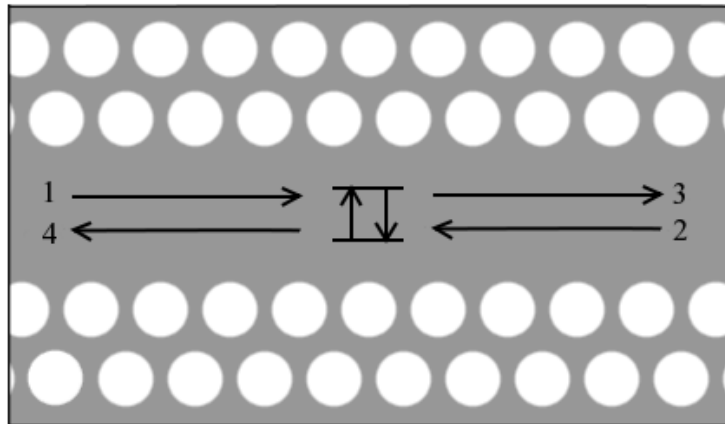
(b) Photonic crystal waveguide

Figure 3.1: (a) An illustration of the four-port beamsplitter arrangement adopted for both the Clauser and Hong-Ou-Mandel experiments with photon detectors placed at the ends of each of the outgoing arms. (b) A 1D channel defect in a periodic 3D photonic crystal will guide light at frequencies otherwise forbidden by an optical band gap. A single two-level emitter placed within the waveguiding structure couples strongly to guided light. The numbering of incoming and outgoing directions on either side of the atom to be compared with (a) makes clear the sense in which it behaves as a beamsplitter in this restricted geometry.
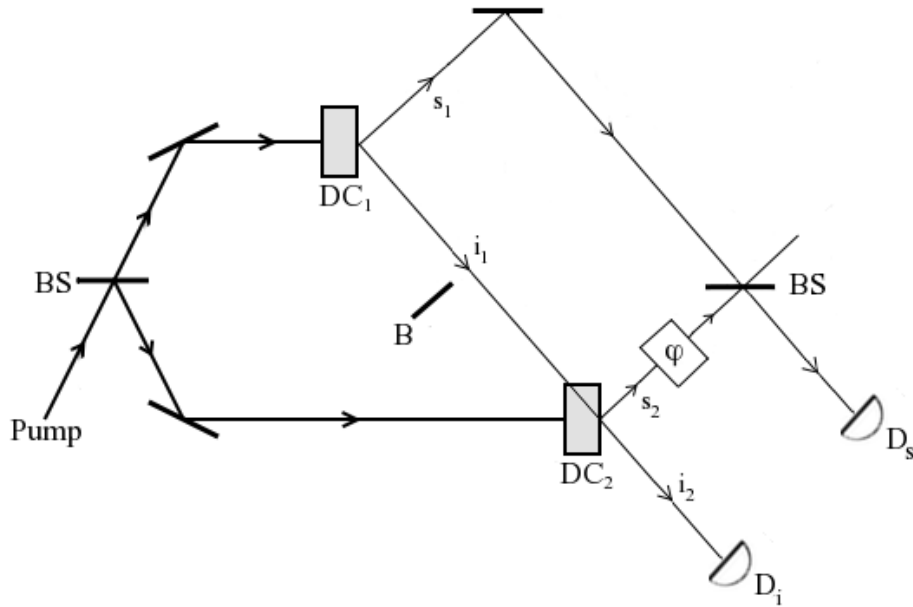
Figure 3.2: A classic experiment performed by Zong, Wang and Mandel [59] illustrating the complementarity principle. A laser beam (pump) is directed at two down-converting crystals that spontaneously generate photon pairs - in so-called signal and idle modes. This process is extremely rare: typically one pair is ejected from each crystal for every 10^{12} incoming photons from the pump field, in other words it is highly unlikely that more than one photon occupies the interferometer during each trial. A signal photon, which may have come from either of the two crystals, travels along s_1 or s_2 and contributes to an interference pattern which is visible after repeated measurements at the detector D_s with different phases φ. These phases are added to the photon state occupying the mode s_2 by adjusting the path length along this route. If the opaque block labelled B is shifted so as to obstruct the path of i_1 then a detection of a photon at D_i indicates that the signal photon in the interferometer must have been generated by the second crystal and interference is lost since which-path information is gained. This is despite the fact that no direct measurements are made on the interfering beams s_1 and s_2.

3.3.1 Photon Counting Statistics

The probability that n photon counts are recorded at one or more detectors, the first made at $\mathbf{r}_1, t_1$ within an interval Δt_1, the second at $\mathbf{r}_2, t_2$ within an interval Δt_2 and so forth is

$$p_n(\mathbf{r}_1, t_1; \ldots; \mathbf{r}_n, t_n)\Delta t_1 \ldots \Delta t_n = \eta_1 \Delta t_1 \cdots \eta_n \Delta t_n \left\langle \mathscr{O}\left[\hat{I}(\mathbf{r}_1, t_1) \cdots \hat{I}(\mathbf{r}_n, t_n)\right]\right\rangle, \qquad (3.11)$$

The above probability generalizes (3.2) to multiple detections [54] where $\mathscr{O}$ performs a normal ordering of creation and annihilation operators while anti-time ordering the creation sector and time ordering annihilation sector so as to properly incorporate the adjustment of the field following each detection.

Photon Bunching and Anti-Bunching

The first observations of the sort (3.11) were recorded by Hanbury Brown and Twiss in the mid 1950s [62] in the field of astronomy. They measured intensity-intensity correlations in the light arriving from the very brightest stars with the aim of determining their size. An unexpected feature in their results was a temporal bunching in the arrival of photons within intervals shorter than the coherence time, $\tau_c = 1/\Delta\omega$ where $\Delta\omega$ is the spectral width of the detected light. Their discovery is often credited as the dawn of experimental quantum optics. The strength of the bunching can be quantified by first writing the two-photon detecton probability in the form

$$p_2(\mathbf{r}_1, t_1; \mathbf{r}_2, t_2)\Delta t_1 \Delta t_2 = g_2(\mathbf{r}_1, t_1; \mathbf{r}_2, t_2)\, p_1(\mathbf{r}_1, t_1)\, p_1(\mathbf{r}_2, t_2)\Delta t_1 \Delta t_2. \qquad (3.12)$$

For a stationary field and with fixed detectors, the probability (3.12) is dependent solely on the delay between detections, $\tau = t_2 - t_1$. The temporal bunching of photons is then indicated by an enhancement in the probability of simultaneous over delayed detections, $g_2(0) > g_2(\tau)$.

This tendency toward bunching is also found in light from many other sources, including thermal sources where the observation is made more challenging by much shorter coherence times [63]. The observation is often attributed to the Bose-statistical exchange effect between identical photons but a straightforward application of the Schwarz inequality reveals that the only restriction for classical probabilities is that $g_2(0) \geqslant g_2(\tau)$ and consequently photon bunching is not in conflict with semi-classical theory [60]. In contrast, anti-bunching which refers to instances when the likelihood of simultaneously detecting two photons is less than the likelihood of delayed detection, $g_2(0) < g_2(\tau)$ can only be interpreted within the context of quantum optics. The quantum character of photon anti-bunching has made it the subject of intense investigation and it has now been observed in a great variety of scenarios, most notably in light resonantly scattered from a two level atom (resonance fluorescence) [19]. The resonance florescence problem will be dealt with more thoroughly in a later chapter where the definition of anti-bunching will be adapted for non-stationary, few-photon pulses.

The probabilities (3.11) are differential and do not normalize to unity when integrated over all times. Time intervals have to be chosen sufficiently small to ensure that the probability of a detection during the specified interval is much less than unity, and any detections that may occur between noncontiguous intervals are not incorporated. A formula for the probability that exactly n photons are detected at $\mathbf{r}$ within $[t, t+\tau]$ in an open system has been derived by Kelly and Kleiner [64]: they find that

$$
P_n(t, t+\tau) = \left\langle \mathscr{O}\left[\frac{\hat{\Omega}^n(t, t+\tau)}{n!} \exp\left[-\hat{\Omega}(t, t+\tau) \right] \right] \right\rangle, \tag{3.13}
$$

where $\hat{\Omega}(t_i, t_j) = \int_{t_i}^{t_j} dt\, \hat{I}(\mathbf{r}, t)$. This result has been used to show that resonantly scattered light from a two level atom is both sub-poissonian and significantly antibunched [65].

3.3.2 The Hong-Ou-Mandel Effect

In this section the classic Hong-Ou-Mandel two-photon interference effect is briefly discussed with particular attention to its purely quantum mechanical origin. This is in preparation for subsequent sections where an extension of the effect to correlated photon pulses will be addressed.

Two identical photons arriving simultaneously from the input ports labelled 1 and 2 of the lossless balanced beamsplitter depicted in figure 3.1a are always found leaving together in only one of the two possible outgoing ports; in particular, counts at both D_3 and D_4 do not occur. The essential physics is illustrated when the incoming state at the beam splitter is characterized in the following way

$$\left| i^2 \right\rangle = |1_1, 1_2\rangle, \tag{3.14}$$

which specifies a configuration with precisely one photon in each incoming port. In this context the action of a symmetric beamsplitter is encoded by a scattering matrix linking incoming photon states to outgoing ones, in general

$$\begin{bmatrix} \hat{a}_3 \\ \hat{a}_4 \end{bmatrix} = \begin{bmatrix} t & r \\ r & t \end{bmatrix} \begin{bmatrix} \hat{a}_1 \\ \hat{a}_2 \end{bmatrix}, \tag{3.15}$$

where $\hat{a}_i$ is the operator responsible for the annihilation of a photon in the ith port. It can be shown, based on the principle of energy conservation alone, that the following reciprocity relations apply [66]

$$|t|^2 + |r|^2 = 1, \quad \bar{r}t + r\bar{t} = 0. \tag{3.16}$$

The joint probability that a photon is detected on each outgoing port is proportional to the average $P_{34} = \langle : \hat{n}_3 \hat{n}_4 : \rangle$ taken over the outgoing state corresponding to (3.14), found with the help of the scattering matrix (3.15) and the above reciprocity relations (3.16):

$$P_{34} = \left(|t|^2 - |r|^2 \right)^2. \tag{3.17}$$

When incident photons are equally likely to be transmitted or reflected, $|t|^2 = |r|^2$, then the probability of joint detection vanishes, $P_{34} = 0$. Interestingly this kind of destructive interference is not found for the coherent incident states $|\alpha_1, \alpha_2\rangle$ irrespective of their intensity. The precise origin of the effect is made especially clear when the outgoing state corresponding to (3.14) is written explicitly,

$$\left| f_i^2 \right\rangle = tr \left| 2_3, 0_4 \right\rangle + rt \left| 0_3, 2_4 \right\rangle + r^2 \left| 1_3, 1_4 \right\rangle + t^2 \left| 1_3, 1_4 \right\rangle. \tag{3.18}$$

For a balanced beamsplitter $r^2 + t^2 = 0$ and the terms that have one photon in each outgoing port mutually cancel. This so-called Hong-Ou-Mandel effect [23] is therefore a consequence of indistinguishability and the resulting quantum interference between photon paths. It is not possible to explain the phenomenon on the basis that each photon interferes only with itself.

In practice single photons are confined to wavepackets of finite duration ($\Delta\tau \sim 15$ fs for those generated in a spontaneous parametric down-conversion (SPDC) crystal for example [23]); they are therefore composed of a range of frequencies and the transmission and reflection properties of a real beamsplitter depend on these incident frequencies (and in some cases even the polarization of each photon). A proper treatment of the Hong-Ou-Mandel effect should take into account these complications. With this aim in mind it is noted that in the original experiment a type-I SPDC is employed to generate the requisite photons. A coherent

laser beam applied to such a nonlinear crystal leads to the spontaneous creation of correlated photon pairs, ejected simultaneously in concentric cones emerging from the crystal about the lasing axis. Photons belonging to each pair are generated with identical polarization and are further entangled by the so-called phase-matching conditions that ensure conservation of energy and momentum (approx.) during each down-conversion process [67]. One consequence of these conditions is that photons belonging to each pair emerge on opposite sides of the emission cones, in so-called signal and idle modes, although the choice of labelling is arbitrary. Apertures and filters are often employed to select photons traveling in particular directions with certain frequency distributions, effectively reducing the description of the problem to one dimension. The relevant class of incoming state can be written in the form

$$\left| i^2 \right\rangle = \int d^2\omega \ C_{\omega,\omega'} \ e^{i(\omega-\omega')\tau/2} \ \hat{a}^+_{\omega,1} \hat{a}^+_{\omega',2} \left| \right\rangle, \tag{3.19}$$

representing two photons (which may have been selected from the signal and idle modes of an SPDC) which have been directed into the incoming ports of a beamsplitter and prepared with relative delay τ. The probability that the photons are later found in distinct outgoing ports, regardless of their frequency, is simply

$$\begin{aligned} P_{34} &= \int d^2\omega \ \left\langle f_i^2 \right| : \hat{n}_{\omega,3} \ \hat{n}_{\omega',4} : \left| f_i^2 \right\rangle, \\ &= \int d^2\omega \ \left| t_\omega t_{\omega'} \ C_{\omega,\omega'} \ e^{i(\omega-\omega')\tau/2} + r_\omega r_{\omega'} \ C_{\omega',\omega} \ e^{-i(\omega-\omega')\tau/2} \right|^2. \end{aligned} \tag{3.20}$$

The spectral entanglement shared by photon pairs generated in an SPDC is not essential for Hong-Ou-Mandel interference; a symmetric joint-frequency distribution for the two-photon state and the equivalence of the transmission and reflection probabilities over the frequency region spanned by the incident photon wavepackets is sufficient. Wavefunctions representing photons with identical frequency distributions but no mutual entanglement factorize, $C_{\omega,\omega'} = g_\omega g_{\omega'}$. Assuming Gaussian distributions with central frequency $\omega_0/2$ and bandwidth $\Delta\omega$ one

obtains the following probability for eventually finding one photon in each outgoing port of an ideal balanced beamsplitter

$$P_{34} = \frac{1}{2}\left(1 - e^{-(\Delta\omega\,\tau)^2/2}\right),\tag{3.21}$$

which has been derived with the assumption that the magnitudes of the transmission and reflection coefficients are equal, $|t_\omega| = |r_\omega| = 1/\sqrt{2}$. The result reveals the characteristic Hong-Ou-Mandel dip corresponding to a complete loss of coincidence counts at zero delay; a qualitatively similar result would have been obtained from the entangled two-photon state generated by an SPDC.

3.4 The Hong-Ou-Mandel Effect with a Single Atom

It follows from the probability (3.21) that the greatest Hong-Ou-Mandel interference is found when two identical photons arrive at a balanced beamsplitter simultaneously. The aim of the current section is to determine the extent to which the strength of the interference is altered when a single two-level atom is used in place of the beamsplitter. The degree of coupling that can be achieved between light and a single dipole in free space is limited by the large density of states available to scattered photons. It was first realised by Purcel [1] that the rate of spontaneous emission of an atom can be enhanced (or suppressed) when it is placed in a resonant (off-resonant) cavity. This led to the wider appreciation that light-matter coupling is often strengthened by reducing the phase-space volume/number of dimensions available for the coupled light to explore. The recent and rapid developments in the field of nano-photonics have provided a great number of ways to achieve this goal. One method that is particularly relevant to the current discussion is photonic waveguiding.

Drawing upon elementary ideas from condensed matter, most notably Bloch's theorem, it

has been shown that sizable one-, two- or even three-dimensional optical band gaps can be generated in photonic crystals by periodically modulating the dielectric constant in the bulk. Defects in these otherwise periodic structures allow many of the forbidden modes to be re-populated in the defected regions. Channel defects are particularly useful because they can operate as waveguides with minimal losses. If the width of such a channel is comparable to the characteristic wavelength of the guided light then the motion of the field in transverse directions is restricted and a one-dimensional continuum is approached. The near-resonant interaction of a single two-level emitter with such a continuum is then well described by the multimode Dicke Hamiltonian for a side-attached impurity

$$\hat{H} = \sum_\sigma \int dk \; \omega_{k,\sigma} \; \hat{a}^+_{k,\sigma}\hat{a}_{k,\sigma} + \sqrt{\gamma} \sum_\sigma \int dk \; (\hat{S}^+\hat{a}_{k,\sigma} + \hat{a}^+_{k,\sigma}\hat{S}^-). \tag{3.22}$$

The first term relates to the free propagation of radiation where all photon energies are referenced with respect to the two-level energy separation ω_{12} and incoming frequencies are assumed quasi-resonant, $|\omega_{k,\sigma} - \omega_{12}| \ll \omega_{12}$. Furthermore, ω_{12} is considered to be well within the optical band gap of the bulk crystal and far from any upper or lower cut-offs for guided frequencies. In the above limits the standard rotating-wave approximation can be made and the coupling of the atom with the field can be replaced by the constant value $\gamma = 4\omega_{12}^3 d/3$ taken at resonance, where d is the magnitude of the dipole matrix element connecting the two atomic levels. The polarization of the incident light is taken to be both linear across all frequencies and parallel to the dipole orientation. It is also implicitly assumed that the typical wavelength of the coupled light is much greater than the atomic dimension.

Since the only active frequencies are those within a narrow region centred on resonance two unrelated chiral modes have been defined, right travelling photons with linear disper-sion, $\omega_{k,R} = v_g k$ where v_g is the (on-resonance) group velocity (which can be appreciably

lower than the speed of light in vacuum) and left traveling photons with $\omega_{k,L} = -v_g k$. The separation of right and left traveling modes is in the same spirit as the linearization of the spectrum that is often performed about the Fermi points for electron liquids in one dimension. Although technically the approximation introduces an infinite number of modes with arbitrarily large negative energies no unphysical artifacts are expected to be incurred since these unphysical modes never become occupied; all scattered photons remain close to resonance.

The Hong-Ou-Mandel geometry is achieved in the current setting if two photons are introduced from each end of the waveguide, are sent toward the atom such that they arrive with some relative delay $\tau = v_g^{-1}\delta$. It is further supposed that there exists a set of frequencies for which the single-photon transmission and reflection probabilities are equal and the frequencies of the incident photons are tuned near to these duality points. The two-level approximation for the atom is valid when the incident light is near resonance with a well isolated dipole transition: in this case only one resonant photon can be absorbed at any given time and the simultaneous processing of both photons that results in the most complete interference is forbidden.

The most direct way to extract the scattering properties from the Hamiltonian (3.22) is by first executing a transformation to modes of even and odd parity, $\hat{a}_{k,\pm} = (\hat{a}_{k,R} \pm \hat{a}_{-k,L})/\sqrt{2}$. In terms of them the Hamiltonian separates:

$$
\begin{aligned}
\hat{H} &= \hat{H}_- + \hat{H}_+ \\
&= \int dk\, v_g k\, \hat{a}_{k,-}^+ \hat{a}_{k,-} + \int dk\, v_g k\, \hat{a}_{k,+}^+ \hat{a}_{k,+} + \sqrt{2\gamma} \int dk\, (\hat{S}^+ \hat{a}_{k,+} + \hat{a}_{k,+}^+ \hat{S}^-).
\end{aligned}
\tag{3.23}
$$

The evolution of photons belonging to the odd-parity modes is straightforward since they do not couple to the atom. Photons in the even modes on the other hand do interact and

their scattering is encoded in the n-photon scattering matrices, $\hat{S}_+^n$, which for one and two photons are given by (2.45) and (2.51) (respectively) with the replacement $\gamma \to 2\gamma$ and the group velocity v_g set to unity.

To illustrate how the known scattering properties of the chiral Dicke model can be used to determine the transmission and reflection amplitudes of the related Hamiltonian (3.22) the state corresponding to a single right-travelling photon impinging on an initially unexcited atom is taken and written in the even-odd representation

$$\left| i_k^1 \right\rangle = \left| k^R \right\rangle = \frac{1}{\sqrt{2}} \left| k^+ \right\rangle + \frac{1}{\sqrt{2}} \left| k^- \right\rangle, \tag{3.24}$$

where the notation $\left| k_n^{\sigma_n}, \ldots, k_1^{\sigma_1} \right\rangle = \hat{a}_{k_n,\sigma_n}^+ \cdots \hat{a}_{k_1,\sigma_1}^+ \left| \right\rangle$ has been adopted for compactness. The evolution of the even sector is then determined by the application of the scattering matrix given in (2.45) while the odd sector remains unaltered, the resulting outgoing state is then

$$\left| f_k^1 \right\rangle = \frac{1}{\sqrt{2}} s_k \left| k^+ \right\rangle + \frac{1}{\sqrt{2}} \left| k^- \right\rangle = t_k \left| k^R \right\rangle + r_k \left| -k^L \right\rangle. \tag{3.25}$$

In the final expression the photon state has been re-represented in terms of the original right and left propagating basis. Comparing the outgoing state (3.25) with (3.24) reveals that an incident right-traveling photon is transmitted with amplitude $t_k = (s_k + 1)/2 = k/(k + i\gamma)$ and reflected with amplitude $r_k = (s_k - 1)/2 = -i\gamma/(k + i\gamma)$. Identical amplitudes would have been obtained for the transmission of a photon through a single resonant energy level (Fano resonance) which is entirely expected since a single resonant photon is insensitive to the finite spectrum of the two-level system.

Equal transmission and reflection probabilities necessary for complete interference are achieved when $k = \pm\gamma$ and since the photon energies are measured with respect to the energy spacing

of the two-level atom the corresponding incident-photon momenta are $\pm v_g^{-1}\omega_0 \pm \gamma$. The goal of the subsequent analysis is to assess the outcome when single photons, arriving from either end of the waveguide, meet the atom with arbitrarily narrow distributions of momenta centred on these duality points. Generalising the previous result (3.25) it can be shown the evolution of a single photon is summarised in the following expression

$$\hat{S}^1 \, |k^\sigma\rangle = \sum_\mu \int dp \, S^{\mu,\sigma}_{p,k} \, |p^\mu\rangle, \qquad (3.26)$$

where the matrix elements are $S^{R,R}_{p,k} = \bar{S}^{L,L}_{p,k} = t_k\delta(k-p)$ and $S^{L,R}_{p,k} = \bar{S}^{R,L}_{p,k} = r_k\delta(k+p)$. In one dimension, scattered and un-scattered light coherently superimpose to form outgoing states; an interesting consequence of the light-atom coupling (3.22) is the total reflection of resonant single photons, $|r_{k=0}|^2 = 1$, despite the comparative smallness of the atom with respect to the light wavelength. This is interpreted in terms of an interference between two Feynman paths: when an incoming photon interacts with an atom that is initially in its ground state the photon receives a delay in propagation encoded in the phase-shift s_k developed by the even sector of the state (3.25). Alternatively the photon passes the emitter without ever interacting and this possibility is recorded by the odd sector. Since the incident photon occupies a mixture of these modes the probability amplitudes for both of these processes combine to give the reflection and transmission coefficients. At resonance the phase shift accumulated by the interacting component is $s_{k=0} = -1$ and consequently the two pathways that lead to transmission mutually cancel leaving reflection as the only remaining possibility.

The evolution of n incident photons can be determined in an analogous way, by representing incoming configurations in terms of their occupation of the even and odd modes and then applying the following scattering matrix that is suited to this basis and easily constructed

61

from the known properties of the chiral Dicke model:

$$\hat{S}^n = \sum_{m=0}^{n} \hat{S}_+^{n-m} \otimes \hat{S}_-^m. \tag{3.27}$$

Since photons in the odd parity modes do not scatter, the matrices $\hat{S}_-^n$ can be replaced by the unit operation. Once the outgoing state is found it can then be re-represented in terms of the original right and left traveling modes. For the following analysis it is more convenient to have the two-photon scattering matrix written in the right-left basis. This is achieved by calculating the evolution of all possible incoming two-photon states; the results are then assembled into the following relation

$$\hat{S}^2 \, |k_2^{\sigma_2}, k_1^{\sigma_1}\rangle = \sum_{\mu_2,\mu_1} \int d^2p \, \left[S_{p_2,k_2}^{\mu_2,\sigma_2} S_{p_1,k_1}^{\mu_1,\sigma_1} + B_{p_2,p_1,k_2,k_1}^{\mu_2,\mu_1,\sigma_2,\sigma_1} \right] |p_2^{\mu_2}, p_1^{\mu_1}\rangle. \tag{3.28}$$

The structure is intuitive: the first term corresponds to independent scattering while the second, entangled contribution is the bound state developed in response to the restrictions placed on the photon dynamics by the finite spectrum of the emitter. The relation (3.28) applies to monochromatic incident photons; a more realistic incoming state incorporates a range of frequencies/momenta, for example

$$|i^2\rangle = \int d^2k \, C_{k_2,k_1}^{\delta} \, |k_2^R, k_1^L\rangle. \tag{3.29}$$

Next, the (pure) state (3.29) together with the representation (3.28) for the evolution of two photons is used to determine the probability that the outgoing photons are found leaving the atom in opposite directions. A suitable choice for the momentum distribution of both photons would be $C_{k_2,k_1}^{\delta} = N_2 \exp(-(k_2-\gamma)^2/2\Delta k^2) \exp(-(k_1+\gamma)^2/2\Delta k^2) \exp(i(k_2+k_1)\delta/2)$ where N_2 is the appropriate normalization constant. In other words the incoming photons are prepared with Gaussian distributions, the right-traveling photon with momentum peaked

at $v_g^{-1}\omega_0 + \gamma$ and the left-traveling photon at $-v_g^{-1}\omega_0 - \gamma$, the widths of both distributions are equivalent and the two photons are separated by an interval $\tau = v_g^{-1}\delta$. It follows from result (3.28) that the outgoing photon state divides naturally into two components

$$\left|f_i^2\right\rangle = \int d^2k \, C_{k_2,k_1}^\delta \left[\left|\mathrm{PW}_{k_2,k_1}\right\rangle + \left|\mathrm{BS}_{k_2,k_1}\right\rangle \right]. \tag{3.30}$$

The first term stems from the independent scattering of both photons and will be called the plane-wave component, the second term is the two-photon bound state. The explicit form of the plane-wave component is

$$\left|\mathrm{PW}_{k_2,k_1}\right\rangle = \sum_\mu \int d^2p \, S_{p_2,k_2}^{\mu_2,R} S_{p_1,k_1}^{\mu_1,L} \left|p_2^{\mu_2}, p_1^{\mu_1}\right\rangle,$$
$$= t_{k_2}\bar{t}_{k_1}\left|k_2^R, k_1^L\right\rangle + r_{k_2}\bar{r}_{k_1}\left|-k_2^L, -k_1^R\right\rangle + t_{k_2}\bar{r}_{k_1}\left|k_2^R, -k_1^R\right\rangle + r_{k_2}\bar{t}_{k_1}\left|-k_2^L, k_1^L\right\rangle$$

$$\tag{3.31}$$

Neglecting the bound-state contribution the probability that the two scattered photons emerge from the emitter traveling in opposite directions is calculated based solely on (3.31):

$$P_{RL}^{PW} = \int d^2k \left| \int d^2p \, C_{p_2,p_1}^\delta \langle k_2^R, k_1^L | \mathrm{PW}_{p_2,p_1} \rangle \right|^2. \tag{3.32}$$

In the limit that $\gamma \gg v_g\Delta k$, when the spectral width of each photon wavepacket is much narrower than the coupling with the emitter a Hong-Ou-Mandel interference equivalent to the result (3.21) is predicted, since in this (quasi-monochromatic) limit the incident photons experience equal transmission and reflection probabilities. Alternatively, when the width of distribution of incoming frequencies greatly exceeds the coupling energy the strength of the interference is eroded by the variation of the transmission and reflection amplitudes with respect to incoming frequencies. The inclusion of the the bound state further deteriorates

the strength of the interference. The precise form of the bound state contribution is

$$
\begin{aligned}
|\mathrm{BS}_{p_2,k_2,p_1,k_1}\rangle &= \int d^2p \sum_{\mu_2,\mu_1} B^{\mu_2,\mu_1,R,L}_{p_2,p_1,k_2,k_1} |p_2^{\mu_2}, p_1^{\mu_1}\rangle \\
&= \frac{1}{4} \int d^2p \left[B_{p_2,-p_1,k_2,-k_1} |P_2^R, P_1^L\rangle + B_{-p_2,p_1,k_2,-k_1} |P_2^L, P_1^R\rangle \right. \\
&\qquad\qquad \left. + B_{p_2,p_1,k_2,-k_1} |P_2^R, P_1^R\rangle + B_{-p_2,-p_1,k_2,-k_1} |P_2^L, P_1^L\rangle \right].
\end{aligned}
\tag{3.33}
$$

Figure 3.4 depicts the probability that two photons that are simultaneously incident ($\delta = 0$) on the atom are later detected traveling in opposite directions. In order to distinguish the reduction of the interference strength due to the frequency dependence of the transmission and reflection amplitudes from that caused by the blockade-like nonlinearity introduced by the emitter, a plot of P_{RL}^{PW} is included. Finally, in the quasi-monochromatic limit, it can be shown that

$$
P_{RL} = \int d^2k \left| \langle k_2^R, k_1^L | f_i^2 \rangle \right|^2 = \frac{1}{2} - \frac{1}{2}\left(1 - \frac{1}{\Gamma}\sqrt{\frac{2}{\pi}} \right) \exp\left(-\Delta^2/2\Gamma^2 \right), \qquad \Gamma \gg 1, \tag{3.34}
$$

where $\Gamma = \gamma/v_g\Delta k$. The above probability highlights the dominance of the nonlinearity of the atom over the imperfectly balanced transmission coefficients at reducing the visibility of the Hong-Ou-Mandel dip.
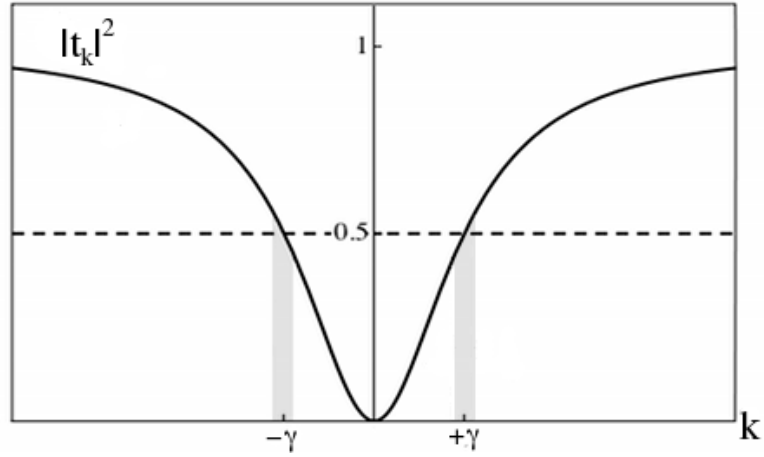
Figure 3.3: The probability of transmission for a monochromatic single photon through a two-level impurity versus incident frequency (relative to the atomic energy level spacing). The narrow bands of frequencies are highlighted near the duality points where the probability of transmission and reflection are approximately equal.
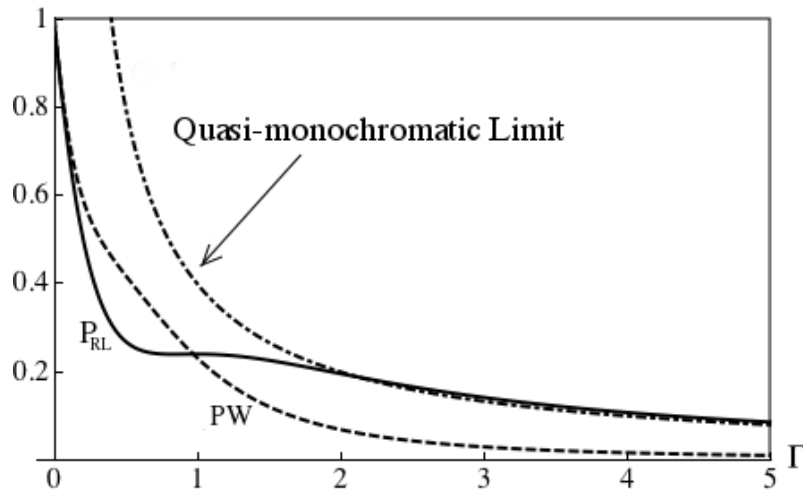
Figure 3.4: The probability that two photons, one incident from either end of the emitter and timed to arrive simultaneously ($\Delta = 0$) are later detected travelling in opposite directions versus the ratio of atom-field coupling to the wavepacket bandwidth. The plane-wave contribution to the probability is given (to illustrate the effects of the frequency dependence of transmission) together with a plot of the full probability in the monochromatic limit.

3.5   Concluding Remarks

In the early part of this chapter various aspects of quantum optical coherence were considered. The general inadequacy of single-photon correlation functions such as the intensity for revealing photon number distributions and effects such as bunching and anti-bunching that has been demonstrated will be important for later work.

In the conventional Hong-Ou-Mandel scenario the probability of the two photons leaving the beamsplitter on separate leads exactly vanishes when they arrive simultaneously. Using the exact scattering states for the Dicke model the loss of interference has been calculated when the single two-level atom assumes the role of a beamsplitter. The loss is appreciable and persists for a large range of coupling strengths.

In a similar study published recently [68] the strength of the Hong-Ou-Mandel visibility is investigated for the scattering of two photons through an on-site impurity with an associated optical nonlinearity. A discretized version of the following model was proposed to model the structure of a saturable impurity and its interaction with the light field

$$\hat{H} = \sum_{\sigma} \int dk \, \omega_k \, \hat{a}_{k,\sigma}^+ \hat{a}_{k,\sigma} + \sqrt{\gamma} \sum_{\sigma} \int dk \, (\hat{b}^+ \hat{a}_{k,\sigma} + \hat{a}_{k,\sigma}^+ \hat{b}^-) + U \, \hat{b}^+ \hat{b} \, (\hat{b}^+ \hat{b} - 1) \qquad (3.35)$$

where $\hat{a}_k$ and $\hat{b}$ mutually commute but obey Bose commutation relations amongst themselves. Apart from the standard reduction of interference visibility associated with the frequency dependence of the transmission and reflection coefficients their numerical investigation also quantified the loss of visibility that stems from the saturation of the impurity. For large nonlinearities, $U \to \infty$, the above Hamiltonian is formally equivalent to the Dicke model, and in this limit their findings agree with ours.

CHAPTER 4

PHOTON BLOCKADE

4.1 Introduction

Photons do not interact directly; instead their interactions have to be mediated by optically nonlinear materials, although the correlations generated between photons in this way are typically very weak. The description of an optically nonlinear device is often reducible to a series of active energy levels: the strongest nonlinearities are then found as the frequency of incident light approaches resonance with any allowed transitions between these levels. It is unfortunate that this increase in nonlinearity on approach to resonance is often accompanied by an enhancement in linear susceptibility. In other words, when the effective interaction between photons is strongest, the single photon absorption and associated loss rate is also maximal and until relatively recently this has been a significant obstacle to the development of all-optical devices.

One of the strongest effective interactions conceivable between photons is a photon blockade, where the absorption of a single control photon by a device is sufficient to prevent the otherwise near-perfect transmission of another. The term photon blockade was introduced by Imamoḡlu et al. [11] (in analogy with the more familiar Coulomb blockade effect found

67

in the charge transport though a mesoscopic quantum dot) in order to describe the lossless giant optical nonlinearities achievable with a particular low-density cavity-confined atomic medium in the regime of electromagnetically-induced transparency (EIT). In this section Coulomb and photon blockade will be introduced and compared and a number of scenarios will be presented where photon blockade has either been observed or predicted. Finally the simplest scheme where photon blockade can be expected is examined, namely two-photon scattering through a single resonantly attached two-level atom. The strength of the blockade in this case is quantified exactly for non-monochromatic incident photons.

4.1.1   Coulomb Blockade

At low temperatures electron transport through a nanoscale metallic island (quantum dot) can exhibit peculiar dependency on a gate voltage capacitevly applied to the dot. Ultimately a regime can be reached where the conductance $g(V_g) = dI/dV_g$ exhibits a series of regular peaks separated by shallow valleys. The phenomenon is understood in terms of the Coulomb repulsion between electrons entering from the leads and those belonging to the island. The spikes in conductivity occur when the gate voltage passes through regions where the energies corresponding to having N and $N + 1$ electrons confined to the island become degenerate. A slightly more quantitative description is provided by considering the electrostatic energy associated with a charge Q on the dot

$$E = QV_g + \frac{1}{2}\frac{Q^2}{C},\tag{4.1}$$

where it is assumed that the coupling to the leads is weak enough that the dot electrons are tightly confined and where the frequency over which electrons are phase coherent greatly exceeds the mean electron energy spacing on the dot. The energy (4.1) is minimal when the charge $Q = Q_0 = -CV_g$. However Q is not a continuous variable, rather it is quantized into

units of the fundamental charge associated with each electron. A mathematical minimum of the energy is therefore only possible when the voltage happens to be some integer multiple of e/C. When the voltage is near one of these degeneracy points, that is $V_g = (N + \delta)e/C$ then

$$E_N = \frac{1}{C}\left(Q(N + \delta)e + \frac{1}{2}Q^2\right), \qquad (4.2)$$

and the difference in energy between having N and $N + 1$ electrons occupying the island is

$$\Delta E = E_{N+1} - E_N = \frac{e^2}{C}\left(\frac{1}{2} - \delta\right). \qquad (4.3)$$

Thus for $\delta < 1/2$ there is an energy penalty - a Coulomb blockade where the electrostatic repulsion between electrons on the island suppresses transmission. Near $\delta \sim 1/2$ the gap is negligible and charge transport proceeds one electron at a time. A substantial review of Coulomb blockade and related phenomena can be found elsewhere [69], the additional spin degree of freedom for electrons leads to much richer physics (including the Kondo effect) than has so far been possible with light.
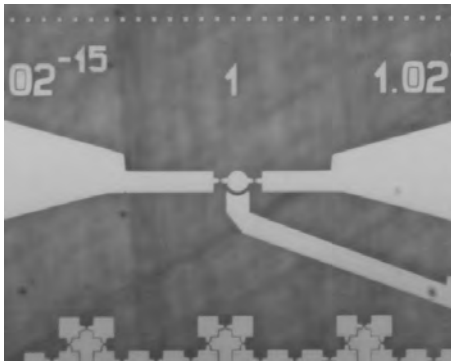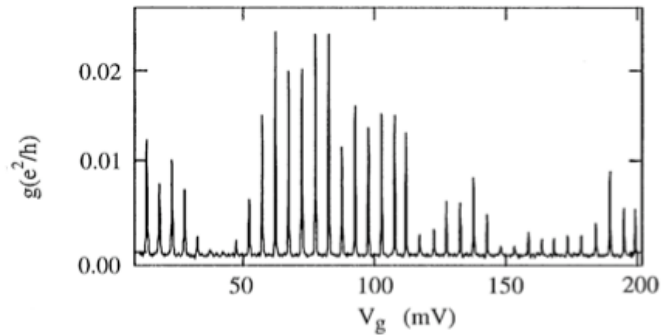
(a) Quantum dot   (b) Coulomb blockade conductance oscillations

Figure 4.1: (a) Optical microscope image of a quantum dot together with leads and gating electrode. (b) Conductance versus gate voltage in the Coulomb blockade regime reproduced from [70].

4.2 Cavity Photon Blockade

One of the most elementary schemes where a photon blockade has been experimentally achieved exploits the anharmonicity of polariton energy levels in an optical cavity containing a single near-resonant two-level emitter. The relevant Hamiltonian in this case is

$$\hat{H} = \omega_{12}\hat{S}^z + (\omega_{12} + \delta\omega)\hat{a}^+\hat{a} + g(\hat{a}^+\hat{S}^- + \hat{S}^+\hat{a}), \tag{4.4}$$

which commutes with operator for the total number of excitations, $\hat{N} = \hat{S}^+\hat{S}^- + \hat{a}^+\hat{a}$ and consequently the Hamiltonian (4.4) can be block-diagonalized; the states associated with each block are the eigenstates of $\hat{N}$ that have the same eigenvalue n. Explicitly, all blocks have the following structure

$$H_n = \begin{bmatrix} \langle e, n-1 | \hat{H} | e, n-1 \rangle & \langle e, n-1 | \hat{H} | g, n \rangle \\ \langle g, n | \hat{H} | e, n-1 \rangle & \langle g, n | \hat{H} | g, n \rangle \end{bmatrix},$$

$$\tag{4.5}$$

$$= (\omega_{12} + \delta\omega)\left(n - \frac{1}{2}\right)\begin{bmatrix} 1 & 0 \\ 0 & 1 \end{bmatrix} + \begin{bmatrix} -\delta\omega/2 & g\sqrt{n} \\ g\sqrt{n} & \delta\omega/2 \end{bmatrix}.$$

The resonant light-atom interaction in the cavity connects the 'bare' states $|e, n-1\rangle$ and $|g, n\rangle$ that correspond to an excited atom with $n - 1$ cavity photons and an unexcited atom with n cavity photons respectively. The result is the formation of dressed states (polaritons) with both photonic and atomic characteristics, denoted by $|n, \pm\rangle$ when $n \geqslant 1$. The energy spectrum of these polaritons follows from (4.5)

$$E_n^{\pm} = (\omega_{12} + \delta\omega)\left(n - \frac{1}{2}\right) \pm \frac{1}{2}\Omega_n, \quad \Omega_n = \sqrt{4g^2n + \delta\omega^2}, \quad n = 1, 2, \ldots \infty. \tag{4.6}$$

70

with the non-degenerate ground state energy, $E_0 = -\omega_{12}/2$. The Hamiltonian is diagonalized by the following transformation

$$\hat{H} = \hat{T}^+ \left[\omega_0 \, \hat{a}^+\hat{a} + (\omega_0 + \Omega_n)\hat{S}^z \right] \hat{T}, \tag{4.7}$$

where $\omega_0 = \omega_{12} + \delta\omega$ is the cavity level spacing in the absence of coupling. The explicit form of the unitary operator $\hat{T}$ is [71]

$$\hat{T} = \exp\left[\hat{j}\,\hat{\theta} \right] = \cos\hat{\theta} + \hat{j}\sin\hat{\theta}, \tag{4.8}$$

The 'angle' of rotation is such that $\sin\hat{\theta} = 2g\hat{N}^{1/2}\,\hat{\Omega}^{-1}$ and $\cos\hat{\theta} = -\delta\omega\,\hat{\Omega}^{-1}$ and where $\hat{j} = \hat{N}^{-1/2}(\hat{S}^+\hat{a} - \hat{a}^+\hat{S}^-)$; with this definition for $\hat{j}$ it is clear that $[\hat{j}, \hat{N}] = 0$ and the following psuedo-complex properties apply; $\hat{j}^2 = -1$, $\hat{j}^+ = -\hat{j}$.

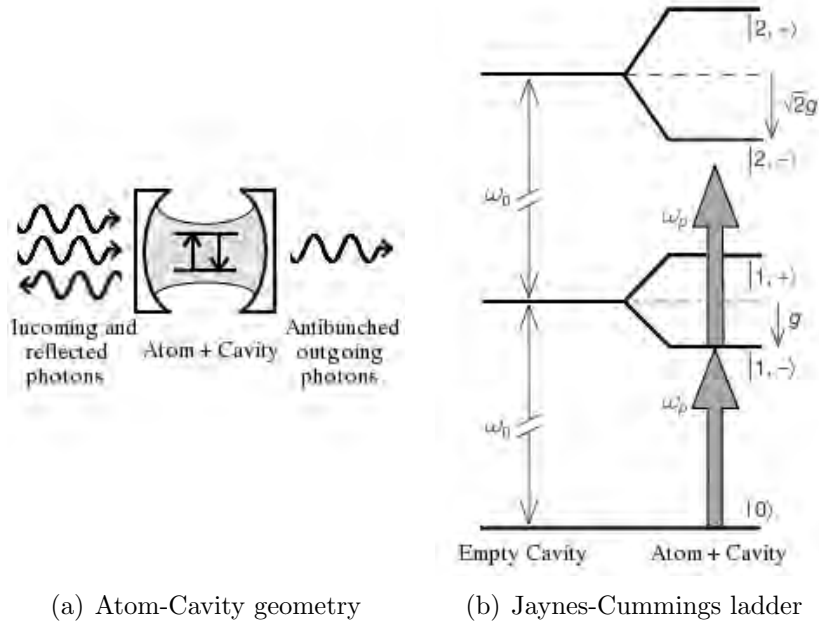(a) Atom-Cavity geometry   (b) Jaynes-Cummings ladder

Figure 4.2: (a) A single atom contained in a resonant optical cavity, in the regime of photon blockade transmitted photons are significantly anti-bunched. (b) The anharmonicity of the Jaynes-Cummings ladder can be exploited to generate a photon blockade.

The foregoing analysis reveals that the otherwise equidistant spacing of energy levels in an empty optical cavity is modified by the introduction of a two-level atom. At resonance the interaction between the cavity modes and the atom lifts the degeneracy between the state containing n cavity photons and an unexcited atom and the state with one less photon and an excited atom. The Jaynes-Cummings Hamiltonian (4.4) has been known, since the early days of quantum optics, to describe a wide range of coherent phenomena including the periodic Rabi-flopping and the spontaneous collapse and revivals of a two-level atom in a resonant cavity [72]. It has been suggested [73] and confirmed experimentally [14] that transmitted light through such a cavity-atom system can exhibit a highly non-classical character. The greatest nonlinearities are expected in the strong-coupling limit when the coupling between the atom and the cavity modes g exceeds both the transverse decay rate of the emitter γ and the loss rate through the cavity walls κ. Ultimately a regime of photon blockade can be reached where light transport through the cavity proceeds one photon at a time.

The energy level diagram in figure 4.2b illustrates how resonant absorption of a single photon with frequency $\omega_p = \omega_0 - g$ to reach the state $|1,-\rangle$ blocks the absorption of another at the same frequency since the transitions to the levels $|2,\pm\rangle$ are detuned from resonance, in other words absorption at ω_p is single photon limited.

In a recent experiment investigating the optical nonlinearities achievable in an optical cavity containing a single trapped two-level atom Birnbaum et al. [14] were able to demonstrate a significant reduction in the value of $g_2(0)$ as compared to $g_2(\tau)$ over a time interval consistent with the lifetime of the state $|2,-\rangle$ responsible for the photon blockade. In addition they found that $g_2(0) \ll 1$ for the transmitted field indicating the conversion (in the context of photon counting statistics) of the incoming Poissonian into outgoing sub-Poissonian light, as depicted in figure 4.3
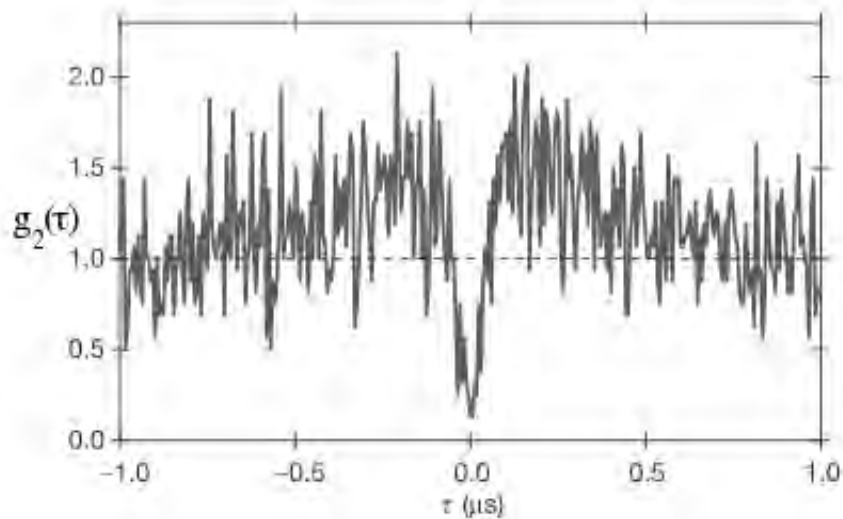
Figure 4.3: Experimental measurement of the second-order intensity correlation function for transmitted light through an optical cavity containing a single caesium atom [14]. The cavity mode is near resonant with the $6S_{1/2}, F = 4 \rightarrow 6P_{3/2}, F' = 5$ transitions, the relevant energies are $(g, \kappa, \gamma)/2\pi = (33.9, 4.1, 2.6)$ MHz. The plot clearly illustrates both photon anti-bunching and sub-Poisonian photon counting statistics. The noise in the signal is associated with the thermal motion of the atom in the cavity ($T \sim 250$ mK).

A complete theoretical picture of light transport through a cavity containing a single two-level atom is now established. Employing a combination of the Lehmann-Symanzik-Zimmermann reduction formalism relating n-body S-matrices to the dynamical Green's functions for the photons and functional-integral techniques, Shi et al. [74] have derived exact expressions for the scattered wavefunctions of one, two and in principle arbitrarily many photons through such an optical cavity+atom embedded in a one-dimensional waveguide geometry. It would be straightforward to use these exact results to calculate the probability for the transmission of incoming few-photon states, and thereby quantify the strength of blockade achievable in this ultra-low intensity limit.

4.3 Photon Blockade with a Resonantly Attached Atom

4.3.1 Resonance Fluorescence

Photon anti-bunching has been predicted for light resonantly scattered from a two-level atom in free space [75], albeit with the scattered photons distributed over the full 4π solid angle. This prediction was later confirmed experimentally in 1977 by the Mandel group [20] by investigating the statistical properties of the scattered light from a beam of sodium atoms irradiated by a frequency and intensity stabilized dye-laser tuned to the particular hyperfine two-level transition ($3P_{3/2}, F = 3, M_F = 2$ to $3^2S_{1/2}, F = 2, M_F = 2$). The intensity of the atomic beam is low enough to ensure that only one atom is irradiated at any given time. It has been shown that for low radiation intensities, when the coupling between the emitter and the field γ greatly exceeds the Rabi frequency Ω, the stationary normalized second-order correlation function fits to

$$g_2(\tau) = \left[1 - \exp\left(-\frac{\gamma\tau}{2}\right)\right]^2, \tag{4.9}$$

whereas in the opposite limit of strong radiation intensities ($\Omega \gg \gamma$).

$$g_2(\tau) = 1 - \exp\left(-\frac{3\gamma\tau}{2}\right)\cos\left(\Omega\tau\right), \tag{4.10}$$

In either regime $g_2(0) < g_2(\tau)$. The above correlation functions can be derived from the Dicke model (2.3) by assuming a resonant, monochromatic coherent state for the incident radiation field. The reduction of the three-dimensional resonance fluorescence problem to only one dimension is accomplished by recognizing that in the context of the dipole approximation it is only necessary to account for s-wave scattering. Although multi-time averages such as the above correlation functions can be calculated using the exact Bethe ansatz wavefunctions [76] little more is gained in comparison to the conventional approach of combining established density matrix techniques with the so-called quantum-regression hypothesis [20, 77].
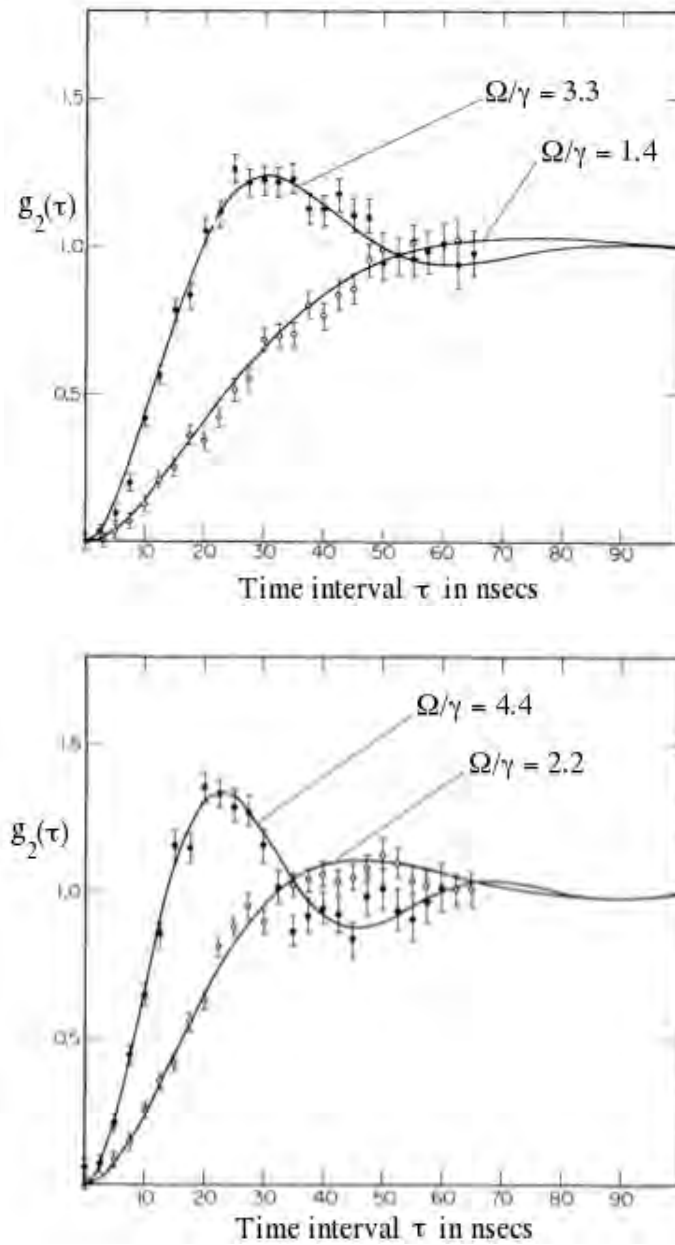
Figure 4.4: A comparison of experimentally determined second-order intensity correlation functions versus delay for various values of incident field intensity (ratio of Rabi frequency to coupling energy) in the resonance fluorescence from a single, coherently irradiated two-level atom. The theoretical predictions are given by the solid curves. Plots taken from Dagenais and Mandel [20].

4.3.2 Blockade with Few-Photon Pulses

Given that photon anti-bunching is known to occur in the context of resonance fluorescence it is perhaps natural to question whether a complete blockade can be achieved with only a couple of incident photons. If the required nonlinearity persists at such low intensities then anti-bunching is expected to be found in the scattered field. One possible way to isolate this purely scattered field would be to resonantly couple the two-level system to two chiral channels that would be otherwise unconnected, for example by placing the atom between two semi-infinite nano-wires each capable of supporting a one-dimensional continuum of surface plasmon modes [4]; this ensures that for any photon to switch leads it must first interact with the atom. Alternatively the reflected light from an atom embedded in a channel waveguide must also have been purely scattered. In either case the relevant Hamiltonian takes the form

$$\hat{H} = \sum_{\sigma} \int dk\, \omega_k\, \hat{a}^+_{k,\sigma}\hat{a}_{k,\sigma} + \sqrt{\gamma}\sum_{\sigma} \int dk\ (\hat{S}^+\hat{a}_{k,\sigma} + \hat{a}^+_{k,\sigma}\hat{S}^-). \tag{4.11}$$

In this chapter we will deal with the so-called resonantly attached geometry where the atom bridges the the gap between two nearby semi-infinite leads which are labeled by, $\sigma = R/L$ depending on whether the lead is to the left or right of the emitter. The surface plasmon dispersion near resonance with the emitter is taken to be $\omega_k = v_g k$. Making a transformation to the modes $\hat{a}_{k,\pm} = (\hat{a}_{k,R}\pm\hat{a}_{k,L})/\sqrt{2}$ decouples the Hamiltonian in a similar fashion to (3.23).

Care should be taken to ensure that the reflection phases acquired as photons reflect from the ends of each lead without interacting with the emitter are accounted for. It can be shown that these bare reflection phases (with a suitable unitary rotation of the field operators) can be shifted to the atomic sector of each eigenstate, and since the contributions to one-time averages from the atomic sector always vanish in the long-time limit these phases can be safely disregarded [79].

4.3.3 Single-Photon Transmission Probability

Just as for the Hong-Ou-Mandel geometry the scattering properties of few-photon states are calculated by representing incoming states in terms of the even and odd modes. The known scattering matrices applied in each sector provide the corresponding outgoing states which can then be re-expressed in terms of the occupation of the right and left leads. Suppose a single photon is incoming from the left lead. In terms of the even and odd basis

$$\left|i_k^1\right\rangle = \left|k^L\right\rangle = \frac{1}{\sqrt{2}}\left|k^+\right\rangle - \frac{1}{\sqrt{2}}\left|k^-\right\rangle, \tag{4.12}$$

applying the single-photon scattering matrix results in the following outgoing state reveals

$$\left|f_k^1\right\rangle = S^1\left|i^1\right\rangle = \frac{1}{\sqrt{2}}s_k\left|k^+\right\rangle - \frac{1}{\sqrt{2}}\left|k^-\right\rangle = t_k\left|k^R\right\rangle + r_k\left|k^L\right\rangle; \tag{4.13}$$

in particular, an incident photon with frequency $v_g^{-1}\omega_0 + k$ will be transmitted with amplitude $t_k = (s_k - 1)/2 = -i\gamma/(k + i\gamma)$ and reflected with amplitude $r_k = (s_k + 1)/2 = k/(k + i\gamma)$ which exposes a duality between the transmission and refection amplitudes for the resonant and anti-resonant geometries. Since any photon is in practice a wavepacket, the probability that the photon is eventually found on the right lead can be calculated explicitly assuming a Gaussian pulse centred on resonance, that is

$$P_R = \int dk \left|\int dp\, C_p \left\langle k^R\left|f_p^1\right\rangle\right.\right|^2 = \int dk\, \left|C_k\, t_k\right|^2 = \sqrt{\pi}\Gamma e^{\Gamma^2}\mathrm{Erfc}(\Gamma). \tag{4.14}$$

with $C_k = N_1 \exp\left(-ak^2/2\right)$ and where $\Gamma = a\gamma = \gamma/v_g\Delta k$ is the dimensionless coupling. The above probability is proportional to the transmitted intensity I_R. When the bulk of the frequencies that contribute to the photon wavepacket are near resonance, which is the case when $\Gamma \gg 1$, then incident photons are almost always transmitted.

4.3.4 Two-Photon Transmission Probability

When two near-resonant photons are incident on a two-level atom from the same lead with some relative delay, then it is expected that the absorption of the leading photon will prevent the absorption and subsequent transmission of the other when the delay between the photons is less than the characteristic decay time of the emitter. The strength of this blockade is quantified by comparing the two-photon transmission probability to the probability that two photons are transmitted independently [47]. The state with two monochromatic photons incident from the left lead on an initially unexcited emitter has the following representation in terms of the even and odd modes

$$\left| i^2_{k_2,k_1} \right\rangle = \left| k_2^L, k_1^L \right\rangle = \frac{1}{2} \left[\left| k_2^+, k_1^+ \right\rangle - \left| k_2^+, k_1^- \right\rangle - \left| k_2^-, k_1^+ \right\rangle + \left| k_2^-, k_1^- \right\rangle \right]; \qquad (4.15)$$

applying the two-photon scattering matrix to the above state provides

$$\left| f^2_{k_2,k_1} \right\rangle = S^2 \left| i^2_{k_2,k_1} \right\rangle = \frac{1}{2} \left[s_{k_2} s_{k_1} \left| k_2^+, k_1^+ \right\rangle - s_{k_2} \left| k_2^+, k_1^- \right\rangle - s_{k_1} \left| k_2^-, k_1^+ \right\rangle + \left| k_2^-, k_1^- \right\rangle \right.$$
$$\left. + \int d^2p \, B_{p_2,p_1,k_2,k_1} \left| p_2^+, p_1^+ \right\rangle \right], \qquad (4.16)$$

which can then be re-written in terms of right-left lead occupation

$$\left| f^2_{k_2,k_1} \right\rangle = t_{k_2} t_{k_1} \left| k_2^R, k_1^R \right\rangle + r_{k_2} t_{k_1} \left| k_2^L, k_1^R \right\rangle + t_{k_2} r_{k_1} \left| k_2^R, k_1^L \right\rangle + r_{k_2} r_{k_1} \left| k_2^L, k_1^L \right\rangle$$
$$+ \frac{1}{4} \sum_{\mu,\mu'} \int d^2p \, B_{p_2,p_1,k_2,k_1} \left| p_2^\mu, p_1^{\mu'} \right\rangle. \qquad (4.17)$$

Neglecting the contribution of the bound state then it follows that two resonant photons would be transmitted entirely, since $\left| t_{k=0} \right|^2 = 1$. Next the probability that both photons are transmitted is calculated assuming that they come with identical Gaussian momentum

distributions and are separated by a delay $\tau = v_g^{-1}\delta$, in this case

$$P_{RR} = \int d^2k \, \frac{1}{2!} \, \Big| \int d^2p \, C^\delta_{p_2,p_1} \, \langle k_2^R, k_1^R \, | f^2_{p_2,p_1} \rangle \Big|^2, \tag{4.18}$$

where $C^\delta_{k_2,k_1} = N_2 \, C_{k_2} C_{k_1} \exp(i(k_2 - k_1)\delta/2)$. It follows that

$$\int d^2p \, C^\delta_{p_2,p_1} \, \langle k_2^R, k_1^R \, | f^2_{p_2,p_1} \rangle = 2C^\delta_{k_2,k_1} t_{k_2} t_{k_1} + \frac{1}{2} \int d^2k' \, C^\delta_{k_2',k_1'} \, B_{k_2',k_1',k_2,k_1}, \tag{4.19}$$

illustrating the plane-wave and bound-state contributions to the transmission probability. The plane-wave component can be determined analytically

$$\begin{aligned} P_{RR}^{PW} &= 2 \int d^2k \, \Big| C^\delta_{k_2,k_1} t_{k_2} t_{k_1} \Big|^2 \\ &= \frac{1}{1 + \exp\left(-\Delta^2/2\Gamma^2\right)} \left[P_R^2 + \frac{\Gamma^2 e^{-\Delta^2/2\Gamma^2}}{4} \left(D_{\Gamma + \Delta/2\Gamma} + D_{\Gamma - \Delta/2\Gamma} \right)^2 \right], \end{aligned} \tag{4.20}$$

where the dimensionless delay is $\Delta = \gamma\delta$ and $D_\Gamma = P_R/\Gamma$. In the limit $\Delta = 0$ the contribution to the probability from the plane-wave sector, P_{RR}^{PW} reduces to independent single-photon scattering, P_R^2. Including the bound state is more tricky to accomplish analytically, however with an exponential parameterization of the delta function the inner product (4.19) can be rewritten as

$$2C^\delta_{k_2,k_1} t_{k_2} t_{k_1} + \frac{1}{\Gamma} \int dx \, (t_{k_2} + t_{k_1}) \, e^{-ia(k_2 + k_1)x} E_{\Delta,\Gamma}(x) \, E_{-\Delta,\Gamma}(x), \tag{4.21}$$

where the following function has been defined due to its ubiquity in subsequent correlation functions

$$\begin{aligned} E_{\Delta,\Gamma}(x) &= \sqrt{\frac{a}{2\pi}} \int dk \, C_k t_k e^{ik(ax + \delta/2)} \\ &= -\frac{\Gamma}{\sqrt{2}} \exp\left[\Gamma^2 + \frac{\Gamma^2}{2} + x\Gamma + \frac{\Delta}{2} \right] \text{Erfc}\left[\frac{1}{\sqrt{2}} \left(\Gamma + x + \frac{\Delta}{2\Gamma} \right) \right]. \end{aligned} \tag{4.22}$$

The contribution to P_{RR} from the bound state alone is then

$$\frac{1}{\Gamma^2} \int d^2k \int d^2x \; |\bar{t}_{k_2} + \bar{t}_{k_1}|^2 \, e^{-ia(k_2+k_1)(x_2-x_1)} E_{\Delta,\Gamma}(x_2) E_{-\Delta,\Gamma}(x_2) E_{\Delta,\Gamma}(x_1) E_{-\Delta,\Gamma}(x_1)$$
$$= \frac{1}{1 + \exp\left(-\Delta^2/2\Gamma^2\right)} \frac{2\pi}{\Gamma} \int dx \; E_{\Delta,\Gamma}^2(x) E_{-\Delta,\Gamma}^2(x).$$

$$(4.23)$$

The cross terms $\bar{t}_{k_2} t_{k_1}$ can be ignored in the integral (4.23) since their poles lie in opposite half planes. The above results can now be combined to give the full two-photon transmission probability

$$P_{RR} = P_{RR}^{PW} + \frac{1}{1 + \exp\left(-\Delta^2/2\Gamma^2\right)} \frac{2\pi}{\Gamma} \int dx \; \Big[E_{\Delta,\Gamma}^2(x) E_{-\Delta,\Gamma}(x) E_{\Delta,\Gamma}(-x)$$
$$+ E_{-\Delta,\Gamma}^2(x) E_{\Delta,\Gamma}(x) E_{-\Delta,\Gamma}(-x) - E_{\Delta,\Gamma}^2(x) E_{-\Delta,\Gamma}^2(x) \Big].$$

$$(4.24)$$

The probability that the lagging photon is transmitted given that the leading photon was also transmitted is then simply P_{RR}/P_R. The strength of the photon blockade is indicated by the ratio of this conditional probability to the single-photon transmission probability P_R. Defining $P_{21} = P_{RR}/P_R^2$ it follows that the blockade is strongest when $P_{21} = 0$; independent photon scattering is identified by $P_{21} = 1$. Figures 4.2 and 4.3 below depict P_{21} versus both delay and coupling strength. Plots of the bound-state ($P_{RR}^{BS} = P_{RR} - P_{RR}^{PW}$) and plane-wave contributions are included. To our knowledge such a calculation has not been made elsewhere.

It might seem intuitive to suppose that the strength of photon blockade is also indicated by the ratio of the two-photon and single-photon transmitted intensities, $I_{21} = I_{RR}/2I_R$ since 'current' correlations such as these are already used as a measure of the strength of Coulomb blockade. Writing the intensity of the transmitted field explicitly in terms of averages over

the quantum state it follows that

$$I_{RR} = \int dk \ \langle f_i^2 | \hat{a}_{k,R}^+ \hat{a}_{k,R} | f_i^2 \rangle = \sum_\sigma \int d^2k \ \langle f_i^2 | \hat{a}_{k_1,R}^+ | k_2^\sigma \rangle \langle k_2^\sigma | \hat{a}_{k_1,R} | f_i^2 \rangle,$$

$$= \int d^2k \ |\langle k_2^R, k_1^R | f_i^2 \rangle|^2 + \int d^2k \ |\langle k_2^L, k_1^R | f_i^2 \rangle|^2 = 2P_{RR} + P_{LR}.$$

(4.25)

and of course, $I_R = P_R$.

Mean transport measurements such as I_{21} however are poor indicators of photon blockade. It was demonstrated in the previous chapter that in optics, first-order correlation functions are insensitive to photon number distributions since they do not distinguish them from the spectral properties of the photon state.

The ratio of two-photon to single-photon transmitted intensities, I_{21} fails most noticeably as an indicator of blockade for weak valises of dimensionless coupling strength and short delays $\Gamma \ll 0.1$ and $\Delta < 1$. Figures 4.7a and 4.7b reveal that I_{12} can be greater than unity (which would naively be taken to indicate bunching) in regions where P_{21}, which is the most reliable of the two measures, indicates blockade, $P_{21} \ll 1$. The failure of the intensity ratio as a measure of blockade can be attributed to Bose-statistical bunching of the incoming photons. Each photon in a symmetrized two-photon state is conditionally more likely to be resonant in comparison to if they were independent. To make this statement more precise, consider the following state describing two photons with temporal delay $\tau = v_g^{-1}\delta$ and identical spectral profiles peaked at resonance

$$|i^2\rangle = \int d^2k \ C_{k_2,k_1}^\delta |k_2, k_1\rangle.$$

(4.26)

From this state it follows that the probability to find one photon with momentum k and another with momentum k' is

$$P_{k,k'} = \left| \langle k, k' \mid i^2 \rangle \right|^2 = \left| C^{\delta}_{k,k'} \right|^2 \tag{4.27}$$

and the probability that at least one photon has momentum k is given by

$$P_k = \int dk \ P_{k,k'} = \int dk \ \left| C^{\delta}_{k,k'} \right|^2 . \tag{4.28}$$

If P_k is interpreted as a single-photon frequency distribution then when the relative delay, δ is finite but less than the width of each photon pulse then the resonant, near $k = 0$ portion of the packet is greater than would it would be if the photon were isolated. The likelihood of any one of the two photons being resonant and subsequently transmitted is therefore enhanced by Bose-statistical bunching. In particular, in the region where blockade is most effective the probability P_{RL} exceeds $P_R P_L$. For this reason the ratio of intensities I_{21} does not adequately quantify blockade.

To conclude this section we note that the effectiveness of the two-level scheme for achieving photon blockade is severely limited by spontaneous emission, no such a limitation is present in Coulomb blockade. The two-level emitter, having accepted a photon does not remain excited indefinitely but instead decays in response to its interaction with vacuum field fluctuations. Maximum photon blockade is achieved when the arrival of the lagging photon is less than the decay time of the emitter, that is $\tau \lesssim \gamma^{-1}$ or written in the dimensionless variables an appreciable blockade is only expected for $\Delta \lesssim 1$, which is confirmed by our findings.

(a) $\Gamma = 0.1$ (b) $\Gamma = 0.3$

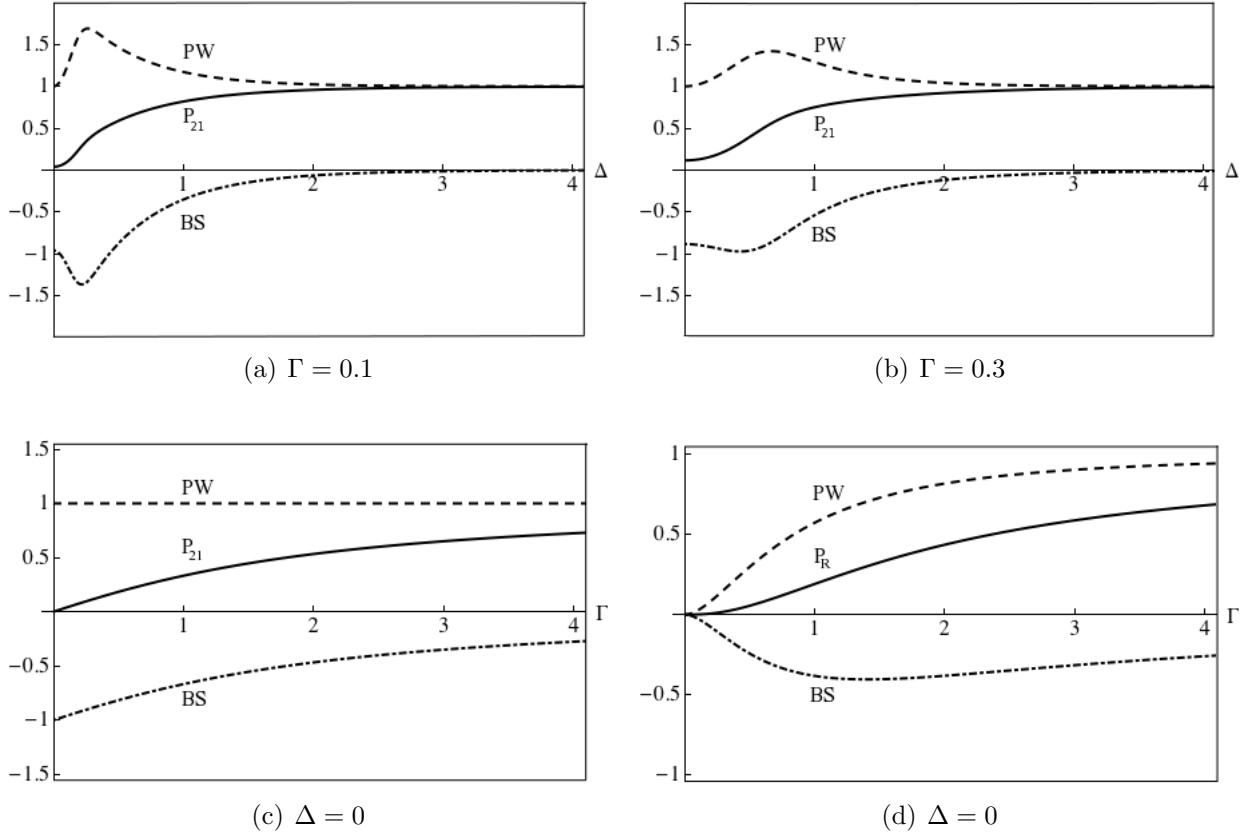(c) $\Delta = 0$ (d) $\Delta = 0$

Figure 4.5: (a)-(b) Strength of blockade versus dimensionless delay between the incoming photons. (c) Blockade strength versus dimensionless coupling at zero delay. (d) Two-photon transmission probability versus dimensionless coupling. Included in each graph are separate plots of the plane-wave and bound-state contributions to the relevant observable.

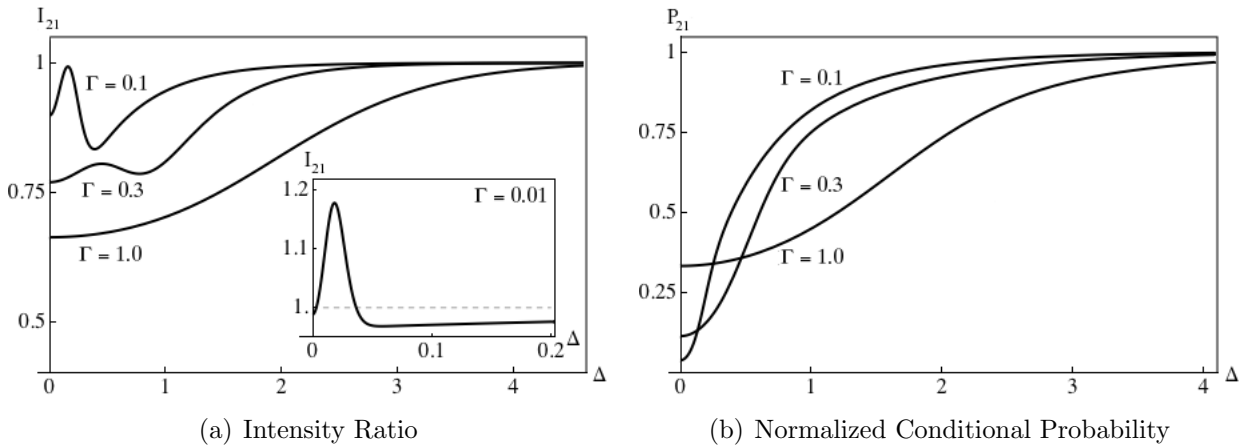(a) Intensity Ratio   (b) Normalized Conditional Probability

Figure 4.6: Comparison between the intensity ratio and normalized conditional probability as indicators of blockade illustrating the failure of the former particularly at weak dimensionless coupling.

83

4.4 Photon Blockade Enhanced by Electromagnetically Induced Transparency

In a pioneering paper by Imamoḡlu et al. [11] it has been suggested that a photon blockade could be achieved in a cavity-confined dilute atomic gas with an associated optical Kerr-type nonlinearity in the regime of electromagnetically-induced-transparency (EIT). Typically a medium becomes opaque to incident radiation at frequencies near to resonance with some optical transition; however, when three or more nearby atomic levels are engaged then it is possible for a destructive interference to develop between the possible excitation pathways, opening up a window of transparency. The utility of EIT stems from the fact that in the region where resonant absorption vanishes the optical nonlinearities may instead undergo a constructive interference [12]. It is these (essentially) absorption-free nonlinearities that are exploited by Imamoḡlu et al. to achieve an efficient photon blockade mechanism.

Ordinarily, the strength of effective photon interactions that can be achieved in a Kerr-nonlinear atomic medium are not sufficiently great for a photon blockade, even with the enhancement offered by EIT. A breakthrough came when Imamoḡlu and Harris [80] noticed that two nearby lifetime-broadened atomic energy levels are formally equivalent to the dressed states formed by a non-perturbative coupling field in resonance with a pair of well-separated energy levels.

Engineering EIT schemes with the aid of non-perturbative coupling fields has been shown to lead to Kerr-type nonlinearities that are many orders of magnitude greater than previously possible with conventional EIT. In particular for the four-level scheme depicted in figure 4.7a it can be shown that a (perturbative) signal field ω_s with Rabi-frequency Ω_s, near resonant with the transition $|2\rangle - |4\rangle$ induces a phase shift in the probe field at ω_p with Rabi-frequency

Ω_p (also perturbative) tuned to $|1\rangle - |2\rangle$ that can be as great as π for only a single incident photon. In addition, the self-phase modulation Kerr-nonlinear coefficients vanish for both the signal and probe fields and the linear susceptibility vanishes for the signal and probe fields in the limit that the decay rate from the state $|2\rangle$ vanishes, $\Gamma_2 = 0$.

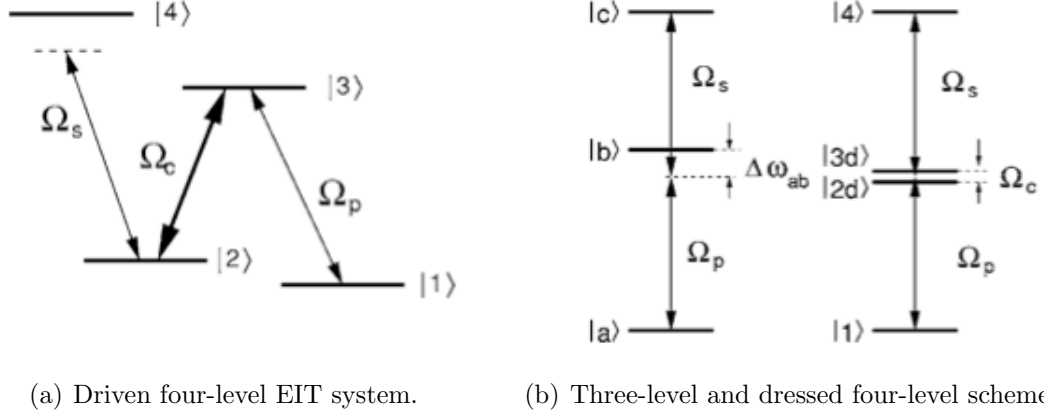(a) Driven four-level EIT system.   (b) Three-level and dressed four-level schemes.

Figure 4.7: (a) A driven four-level system exhibiting both EIT and a giant cross-phase Kerr-nonlinearity between the perturbative pump and signal fields. (b) Left: Three-level EIT scheme. Right: Driven four-level scheme in dressed-state picture [12].

To gain some insight into the enhancement in nonlinearity achievable with the coherently driven 4-level scheme its strength will be compared to that generated by the 3 levels (which also exhibit EIT) depicted on the left-hand-side of figure 4.7b. By expanding the atomic polarizability to third order in the electric field it can be shown (for a dilute gas) that the self-phase Kerr-coefficients for the three-level scheme do not vanish and that the real part of the cross-phase Kerr-nonlinearities in both cases are as follows [12]

$$\text{Re}\left\{\chi_{4-\text{level}}^{(3)}\right\} = \frac{|\mu_{13}|^2 |\mu_{24}|^2 \rho}{2\varepsilon_0 \hbar^3} \frac{1}{\Omega_c^2 \Delta\omega_{42}^2}. \tag{4.29}$$

where μ_{ij} and $\Delta\omega_{ij}$ are the dipole matrix elements of and detuning between the transition $|i\rangle$-$|j\rangle$ and ρ is the atomic number density. For 3 levels without any classical pumping field

(analogous to Ω_c) the real part of the cross-phase third order susceptibility is

$$\text{Re}\left\{\chi^{(3)}_{3-\text{level}}\right\} = \frac{|\mu_{ab}|^2 |\mu_{bc}|^2 \rho}{2\varepsilon_0 \hbar^3} \frac{1}{\Delta\omega_{ab}^2 \Delta\omega_{bc}}. \tag{4.30}$$

The two coefficients are almost identical except the replacement of $\Delta\omega_{ab}$ by Ω_c in going from three-levels to four (with coherent pumping). Whereas for three levels it is necessary that $\Delta\omega_{ab}^2 \geqslant \Gamma_b^2$ to avoid absorption, no such limit exists in the driven four-level scheme, which is the key reason that stronger effective photon interactions can be achieved there.

A classically pumped dilute gas of four-level atoms (see figure 4.7a) when confined to an optical cavity with optical finesse $F \sim 10^4$ is expected to exhibit nonlinearities that are as much as 10 orders of magnitude greater than have previously been thought possible [11]. In this regime the transmission of light through the cavity is predicted to be one-photon limited and the following effective Hamiltonian (after adiabatically eliminating the atomic degrees of freedom) is derived for the light transport

$$\hat{H} = \left(\omega_{\text{cav}} - i\frac{g}{2}\right)\hat{a}^+\hat{a} + \sqrt{2g}(\beta^*\hat{a} + \hat{a}^+\beta) + U\hat{a}^+\hat{a}^+\hat{a}\,\hat{a}, \tag{4.31}$$

where ω_0 is the cavity mode frequency, β is the classical driving field and $\hat{a}$ is the cavity mode photon annihilation operator. The above Hamiltonian is reminiscent of the Coulomb blockade problem where the nonlinearity

$$U = \frac{3\,\omega_{\text{cav}}^2}{2\varepsilon_0 V_{\text{cav}}}\text{Re}\left\{\chi^{(3)}_{4-\text{level}}\right\} \tag{4.32}$$

replaces the 'charging energy'. It has subsequently been pointed out that the elimination of atomic variables above imposes additional, rather stringent limits on the coupling strength that is required for blockade [81]. This problem is overcome when only a single atom is used.

86

More recently few-photon transport through a single driven four-level atom (as above) has been considered in a one-dimensonal photonic waveguide setting [47]. In this case the strength of the photon blockade, P_{21}, is determined numerically for simultaneously incident two-photon pulses near resonance with both the $|1\rangle - |2\rangle$ and $|3\rangle - |4\rangle$ transitions. It is found that P_{12} monotonically increases with coupling strength despite being in the EIT regime.

4.5   Conclusions

One of the key purposes of the preceding chapter was to introduce a number of existing schemes where photon blockade has been predicted and or detected. The strength of photon blockade is defined and calculated for two photons resonantly transmitted through a single two-level atom. The blockade in this setting is severely inhibited by the competing process of spontaneous emission; a reasonable blockade is only achieved for photon delays much shorter than the typical atom decay time.

The advantages of working with a multi-level emitter for generating blockade has also been discussed, in particular the absorption-free giant optical nonlinearities that can be achieved in the regime of electromagnetic-induced-transparency. Few photon transport has been recently investigated in this setting. If the optical nonlinearities offered by single emitters interacting with few photon states are to be exploited in the field of quantum computing then it will almost certainly be necessary to shift beyond two-level schemes.

LIST OF REFERENCES

[1] E. Purcell, "Spontaneous emission probabilities at radio frequencies," *Phys. Rev.*, vol. 69, p. 681, 1946.

[2] W. Barnes, A. Dereux, T. Ebbesen, *et al.*, "Surface plasmon subwavelength optics," *Nature*, vol. 424, no. 6950, pp. 824–830, 2003.

[3] J. Ye, D. Vernooy, and H. Kimble, "Trapping of single atoms in cavity qed," *Physical Review Letters*, vol. 83, no. 24, pp. 4987–4990, 1999.

[4] D. Chang, A. Sørensen, P. Hemmer, and M. Lukin, "Quantum optics with surface plasmons," *Physical review letters*, vol. 97, no. 5, p. 53002, 2006.

[5] J. Joannopoulos, P. Villeneuve, and S. Fan, "Photonic crystals: putting a new twist on light," *Nature*, vol. 386, no. 6621, pp. 143–149, 1997.

[6] T. Ladd, F. Jelezko, R. Laflamme, Y. Nakamura, C. Monroe, and J. O'Brien, "Quantum computers," *Nature*, vol. 464, no. 7285, pp. 45–53, 2010.

[7] W. Munro, K. Nemoto, and T. Spiller, "Weak nonlinearities: a new route to optical quantum computation," *New Journal of Physics*, vol. 7, p. 137, 2005.

[8] J. O'Brien, "Optical quantum computing," *Science*, vol. 318, no. 5856, pp. 1567–1570, 2007.

[9] N. Imoto, H. Haus, and Y. Yamamoto, "Quantum nondemolition measurement of the photon number via the optical kerr effect," *Physical Review A*, vol. 32, no. 4, p. 2287, 1985.

[10] W. Munro, K. Nemoto, R. Beausoleil, and T. Spiller, "A high-efficiency quantum non-demolition single photon number resolving detector," *Arxiv preprint quant-ph/0310066*, 2003.

[11] A. Imamoḡlu, H. Schmidt, G. Woods, and M. Deutsch, "Strongly interacting photons in a nonlinear cavity," *Phys. Rev. Lett.*, vol. 79, pp. 1467–1470, Aug 1997.

[12] M. Fleischhauer, A. Imamoglu, and J. P. Marangos, "Electromagnetically induced transparency: Optics in coherent media," *Rev. Mod. Phys.*, vol. 77, pp. 633–673, Jul 2005.

[13] D. Chang, A. Sørensen, E. Demler, and M. Lukin, "A single-photon transistor using nanoscale surface plasmons," *Nature Physics*, vol. 3, no. 11, pp. 807–812, 2007.

[14] K. Birnbaum, A. Boca, R. Miller, A. Boozer, T. Northup, and H. Kimble, "Photon blockade in an optical cavity with one trapped atom," *Nature*, vol. 436, no. 7047, pp. 87–90, 2005.

[15] C. Lang, D. Bozyigit, C. Eichler, L. Steffen, J. Fink, A. Abdumalikov Jr, M. Baur, S. Filipp, M. da Silva, A. Blais, *et al.*, "Observation of resonant photon blockade at microwave frequencies using correlation function measurements," *Physical Review Letters*, vol. 106, no. 24, p. 243601, 2011.

[16] I. I. Smolyaninov, A. V. Zayats, A. Gungor, and C. C. Davis, "Single-photon tunneling via localized surface plasmons," *Phys. Rev. Lett.*, vol. 88, p. 187402, Apr 2002.

[17] B. Dayan, A. Parkins, T. Aoki, E. Ostby, K. Vahala, and H. Kimble, "A photon turnstile dynamically regulated by one atom," *Science*, vol. 319, no. 5866, pp. 1062–1065, 2008.

[18] A. Imamoglu and Y. Yamamoto, "Turnstile device for heralded single photons: Coulomb blockade of electron and hole tunneling in quantum confined p - i - n heterojunctions," *Phys. Rev. Lett.*, vol. 72, pp. 210–213, Jan 1994.

[19] H. J. Kimble, M. Dagenais, and L. Mandel, "Photon antibunching in resonance fluorescence," *Phys. Rev. Lett.*, vol. 39, pp. 691–695, Sep 1977.

[20] M. Dagenais and L. Mandel, "Investigation of two-time correlations in photon emissions from a single atom," *Phys. Rev. A*, vol. 18, pp. 2217–2228, Nov 1978.

[21] R. Dicke, "Coherence in spontaneous radiation processes," *Physical Review*, vol. 93, no. 1, p. 99, 1954.

[22] V. I. Yudson and P. Reineker, "Multiphoton scattering in a one-dimensional waveguide with resonant atoms," *Phys. Rev. A*, vol. 78, p. 052713, Nov 2008.

[23] C. Hong, Z. Ou, and L. Mandel, "Measurement of subpicosecond time intervals between two photons by interference," *Physical Review Letters*, vol. 59, no. 18, pp. 2044–2046, 1987.

[24] M. Frasca, "A modern review of the two-level approximation," *Annals of Physics*, vol. 306, no. 2, pp. 193–208, 2003.

[25] H. Bethe, "Zur theorie der metalle," *Z. Phys*, vol. 71, p. 205, 1931.

[26] E. H. Lieb and W. Liniger, "Exact analysis of an interacting bose gas. i. the general solution and the ground state," *Phys. Rev.*, vol. 130, pp. 1605–1616, May 1963.

[27] H. B. Thacker, "Exact integrability in quantum field theory and statistical systems," *Rev. Mod. Phys.*, vol. 53, pp. 253–285, Apr 1981.

[28] V. I. Rupasov, "Contribution to the dicke superradiance theory. exact solution of the quasi-one-dimensional quantum model," *Sov. Phys. JETP*, vol. 83, pp. 1711–1723, 1982.

[29] P. Mehta and N. Andrei, "Nonequilibrium transport in quantum impurity models: The bethe ansatz for open systems," *Phys. Rev. Lett.*, vol. 96, p. 216802, Jun 2006.

[30] C. N. Yang, "Some exact results for the many-body problem in one dimension with repulsive delta-function interaction," *Phys. Rev. Lett.*, vol. 19, pp. 1312–1315, Dec 1967.

[31] R. Baxter, "Partition function of the eight-vertex lattice model," *Annals of Physics*, vol. 70, no. 1, pp. 193–228, 1972.

[32] R. Baxter, *Exactly solved models in statistical mechanics*, vol. 9. Academic press London, 1982.

[33] V. I. Rupasov and V. I. Yudson, "Rigourous theory of cooperasive spontaneous emission of radiation from a lumped system of two-level atoms: Bethe ansatz method," *Sov. Phys. JETP*, vol. 60, p. 927, November 1984.

[34] P. Wiegmann, "Exact solution of the sd exchange model (kondo problem)," *Journal of Physics C: Solid State Physics*, vol. 14, p. 1463, 1981.

[35] P. Wiegmann and A. Tsvelick, "Exact solution of the anderson model: I," *Journal of Physics C: Solid State Physics*, vol. 16, p. 2281, 1983.

[36] J.-T. Shen and S. Fan, "Strongly correlated two-photon transport in a one-dimensional waveguide coupled to a two-level system," *Phys. Rev. Lett.*, vol. 98, p. 153003, Apr 2007.

[37] J.-T. Shen and S. Fan, "Strongly correlated multiparticle transport in one dimension through a quantum impurity," *Phys. Rev. A*, vol. 76, p. 062709, Dec 2007.

[38] V. I. Rupasov and V. I. Yudson, "Dicke superradiance theory: Bethe wavefunctions in the discrete atom model," *Sov. Phys. JETP*, vol. 59, p. 478, March 1984.

[39] V. I. Yudson, "Dynamics of quantum integrable systems," *Sov. Phys. JETP*, vol. 61, p. 1043, May 1985.

[40] B. Lippmann and J. Schwinger, "Variational principles for scattering processes. i," *Physical Review*, vol. 79, no. 3, p. 469, 1950.

[41] L. L. Foldy and W. Tobocman, "Application of formal scattering theory to many-body problems," *Phys. Rev.*, vol. 105, pp. 1099–1100, Feb 1957.

[42] J. Taylor and H. Uberall, "Scattering theory: The quantum theory of nonrelativistic collisions," *Physics Today*, vol. 26, p. 55, 1973.

[43] I. Sigal and A. Soffer, "Asymptotic completeness of multiparticle scattering," *Differential Equations and Mathematical Physics*, pp. 435–472, 1987.

[44] M. Pletyukhov and V. Gritsev, "Scattering of massless particles in one-dimensional chiral channel," *New J.Phys.*, vol. 14, p. 095028, 2012.

[45] V. Korepin, "Calculation of norms of bethe wave functions," *Communications in Mathematical Physics*, vol. 86, no. 3, pp. 391–418, 1982.

[46] T. Newton and E. Wigner, "Localized states for elementary systems," *Reviews of Modern Physics*, vol. 21, no. 3, p. 400, 1949.

[47] H. Zheng, D. J. Gauthier, and H. U. Baranger, "Waveguide qed: Many-body bound-state effects in coherent and fock-state scattering from a two-level system," *Phys. Rev. A*, vol. 82, p. 063816, Dec 2010.

[48] S. Fan, E. Kocabas, and J.-T. Shen, "Input-output formalism for few-photon transport in one-dimensional nanophotonic waveguides coupled to a qubit," *Phys. Rev. A*, vol. 82, p. 063821, Dec 2010.

[49] C. W. Gardiner and M. J. Collett, "Input and output in damped quantum systems: Quantum stochastic differential equations and the master equation," *Phys. Rev. A*, vol. 31, pp. 3761–3774, Jun 1985.

[50] K. J. Blow, R. Loudon, S. J. D. Phoenix, and T. J. Shepherd, "Continuum fields in quantum optics," *Phys. Rev. A*, vol. 42, pp. 4102–4114, Oct 1990.

[51] A. Einstein, "Zum gegenwärtigen stand des strahlungsproblems," *Physikalische Zeitschrift*, vol. 10, pp. 185–193, 1909.

[52] R. Glauber, "Coherent and incoherent states of the radiation field," *Physical Review*, vol. 131, no. 6, pp. 2766–2788, 1963.

[53] P. Dirac, "The principles of quantum mechanics," *The International Series of Monographs on Physics, Oxford: Clarendon Press, 1947*, vol. 1, 1947.

[54] L. Mandel and E. Wolf, *Optical coherence and quantum optics*. Cambridge Univ Pr, 1995.

[55] R. J. Glauber, "The quantum theory of optical coherence," *Phys. Rev.*, vol. 130, pp. 2529–2539, Jun 1963.

[56] M. Kitagawa, N. Imoto, and Y. Yamamoto, "Realization of number-phase minimum-uncertainty states and number states by quantum nondemolition measurement," *Phys. Rev. A*, vol. 35, pp. 5270–5273, Jun 1987.

[57] L. Mandel, "Coherence and indistinguishability," *Optics letters*, vol. 16, no. 23, pp. 1882–1883, 1991.

[58] L. Mandel, "Quantum effects in one-photon and two-photon interference," *Rev. Mod. Phys*, vol. 71, no. 2, pp. S274–S282, 1999.

[59] X. Zou, L. Wang, and L. Mandel, "Induced coherence and indistinguishability in optical interference," *Physical review letters*, vol. 67, no. 3, pp. 318–321, 1991.

[60] C. Gerry, P. Knight, and M. Beck, "Introductory quantum optics.," *American Journal of Physics*, vol. 73, p. 1197, 2005.

[61] P. Grangier, G. Roger, and A. Aspect, "Experimental evidence for a photon anticorrelation effect on a beam splitter: a new light on single-photon interferences," *EPL (Europhysics Letters)*, vol. 1, p. 173, 1986.

[62] R. Brown and R. Twiss, "Interferometry of the intensity fluctuations in light. i. basic theory: the correlation between photons in coherent beams of radiation," *Proceedings of the Royal Society of London. Series A. Mathematical and Physical Sciences*, vol. 242, no. 1230, pp. 300–324, 1957.

[63] B. L. Morgan and L. Mandel, "Measurement of photon bunching in a thermal light beam," *Phys. Rev. Lett.*, vol. 16, pp. 1012–1015, May 1966.

[64] P. Kelley and W. Kleiner, "Theory of electromagnetic field measurement and photoelectron counting," *Phys. Rev*, vol. 136, no. 2A, pp. A316–A334, 1964.

[65] L. Mandel, "Sub-poissonian photon statistics in resonance fluorescence," *Optics Letters*, vol. 4, no. 7, pp. 205–207, 1979.

[66] Z. Ou and L. Mandel, "Derivation of reciprocity relations for a beam splitter from energy balance," *American Journal of Physics*, vol. 57, pp. 66–67, 1989.

[67] D. C. Burnham and D. L. Weinberg, "Observation of simultaneity in parametric production of optical photon pairs," *Phys. Rev. Lett.*, vol. 25, pp. 84–87, Jul 1970.

[68] P. Longo, J. Cole, and K. Busch, "The hong-ou-mandel effect in the context of few-photon scattering," *Optics Express*, vol. 20, no. 11, pp. 12326–12340, 2012.

[69] C. W. J. Beenakker, "Theory of coulomb-blockade oscillations in the conductance of a quantum dot," *Phys. Rev. B*, vol. 44, pp. 1646–1656, Jul 1991.

[70] I. Aleiner, P. Brouwer, and L. Glazman, "Quantum effects in coulomb blockade," *Physics Reports*, vol. 358, no. 5-6, pp. 309–440, 2002.

[71] P. Carbonaro, G. Compagno, and F. Persico, "Canonical dressing of atoms by intense radiation fields," *Physics Letters A*, vol. 73, no. 2, pp. 97–99, 1979.

[72] N. B. Narozhny, J. J. Sanchez-Mondragon, and J. H. Eberly, "Coherence versus incoherence: Collapse and revival in a simple quantum model," *Phys. Rev. A*, vol. 23, pp. 236–247, Jan 1981.

[73] A. Auffèves-Garnier, C. Simon, J.-M. Gérard, and J.-P. Poizat, "Giant optical nonlinearity induced by a single two-level system interacting with a cavity in the purcell regime," *Phys. Rev. A*, vol. 75, p. 053823, May 2007.

[74] T. Shi, S. Fan, and C. P. Sun, "Two-photon transport in a waveguide coupled to a cavity in a two-level system," *Phys. Rev. A*, vol. 84, p. 063803, Dec 2011.

[75] H. J. Kimble and L. Mandel, "Theory of resonance fluorescence," *Phys. Rev. A*, vol. 13, pp. 2123–2144, Jun 1976.

[76] V. Rupasov and V. Yudson, "Multi-particle scattering problem in the integrable quantum bloch-maxwell model," *Institute of Spectroscopy, Troitsk*, vol. 26, 1987.

[77] G. S. Agarwal, "Time factorization of the higher-order intensity correlation functions in the theory of resonance fluorescence," *Phys. Rev. A*, vol. 15, pp. 814–816, Feb 1977.

[78] B. R. Mollow, "Power spectrum of light scattered by two-level systems," *Phys. Rev.*, vol. 188, pp. 1969–1975, Dec 1969.

[79] J.-T. Shen and S. Fan, "Theory of single-photon transport in a single-mode waveguide. i. coupling to a cavity containing a two-level atom," *Phys. Rev. A*, vol. 79, p. 023837, Feb 2009.

[80] A. Imamoğlu and S. Harris, "Lasers without inversion: interference of dressed lifetime-broadened states," *Optics letters*, vol. 14, no. 24, pp. 1344–1346, 1989.

[81] P. Grangier, D. F. Walls, and K. M. Gheri, "Comment on "strongly interacting photons in a nonlinear cavity"," *Phys. Rev. Lett.*, vol. 81, pp. 2833–2833, Sep 1998.